Association of PCSK9 with low density lipoproteins (LDL) in the regulation of LDL-cholesterol levels

SAMANTHA KHADIJA SARKAR

Thesis submitted to the Faculty of Graduate and Postdoctoral Studies

In partial fulfillment of the requirements

For the degree of

Master of Science

Department of Biochemistry, Microbiology and Immunology

University of Ottawa

Ottawa, Ontario, Canada

Abstract

Proprotein Convertase Subtilisin / Kexin Type-9 (PCSK9) has emerged as a major regulator of plasma cholesterol levels. PCSK9 is secreted mainly from the liver and circulates as a plasma protein. PCSK9 binds cell surface low-density lipoprotein (LDL) receptors and mediates their degradation upon endocytosis in the liver. This decreases the liver's ability to clear LDL-cholesterol from the blood. PCSK9 is also capable of binding LDL particles themselves; this interaction inhibits the ability of PCSK9 to bind and mediate LDLR degradation in cultured hepatic cells, but its effect on PCSK9 function in vivo remains unknown. A disordered N-terminal region of the PCSK9 prodomain is necessary for binding to isolated LDL particles in vitro. This N-terminal region is also autoinhibitory to PCSK9-LDL receptor binding. We hypothesized that the N-terminal of the PCSK9 prodomain plays a role in an allosteric mechanism that regulates PCSK9 function. Through mutagenesis studies, we found that both a conserved stretch of acidic residues and an adjacent conserved stretch of hydrophobic residues are crucial for the PCSK9-LDL interaction; the hydrophobicity of the residue at position 38 (Tyr) within the conserved acidic stretch was also found to be important for this. Helical wheel modeling of the prodomain N-terminal sequence revealed the potential for a lipid-ordered amphipathic helix to form, which may aid PCSK9 docking onto LDL. Replacing residues A44 and L41 with helix-disrupting proline residues abolished LDL binding. Co-pelleting ultracentrifugation assays also show that wild-type PCSK9 is capable of associating with liposomes, while the A44P mutation disrupts this lipid association. The A44P-PCSK9 mutation, showing an 80-90% decrease in LDL association but with LDL receptor binding and degrading functions intact, may serve as an important tool in future studies investigating the PCSK9-LDL interaction in vivo. Elucidation of the mechanism by which LDL-binding naturally inhibits PCSK9 activity may also help to develop new anti-PCSK9 therapeutics in the future.

Acknowledgements

It takes a village to raise a child, and as a beginner in the study of scientific research, I have been lucky enough to have a wonderful village to "raise" me throughout the journey that has led to this thesis.

Firstly, I am grateful to my supervisor, Dr. Thomas Lagace, for the opportunity to work with him, and for the constant guidance and support. His patience in scientific teaching has been invaluable; however it is his firm direction and encouragement in the face of difficult or discouraging experiments that really brought my work to fruition. Thanks also to my Thesis Advisory Committee members Dr. Ruth McPherson and Dr. Alex Stewart, for their valuable feedback on my project.

I have been very lucky to be part of the lovely community on the 4th floor of the Heart Institute, where helping hands are never hard to come by. I must especially express gratitude to those who have helped me the most in facing the daily challenges of working in a lab. Past lab members such as Dr. Mia Golder and Geoffrey Leblond contributed greatly to my training and my project in the beginning. Special thanks must be given to Tanja Kosenko. Her ever-present readiness to sit down with me and analyze experimental results or help me with technical troubleshooting will always be appreciated.

There are of course, the steadfast friends who helped maintain my sanity throughout the process - or rather, helped to chase down my runaway sanity and bring it back every time I lost it. They know who they are.

Most of all, I am grateful to my parents. Their contribution to my achievements can never be expressed in words.

Contents

List of Abbreviations

ADH	Autosomal dominant hypercholesterolemia
ApoA / B / C	Apolipoprotein A / B / C
ApoB100	Apolipoprotein B100
ARH	Autosomal recessive hypercholesterolemia
CETP	Cholesteryl ester transfer protein
CHD	Coronary heart disease
CTD	C terminal domain
CVD	Cardiovascular disease
DMEM	Dulbecco's modified eagle's medium
DNA	Deoxyribonucleic acid
dNTP	Deoxyribonucleotide
DOPC	1,2-dioleoyl-sn-glycero-3-phosphocholine
DOPE	1,2-dioleoyl-sn-glycero-3-phosphoethanolamine
EGF	Epidermal growth factor-like
ER	Endoplasmic reticulum
FBS	Fetal bovine serum
HBSC	HEPES-buffered saline with calcium
HDL	High density lipoprotein
HEK293	Human embryonic kidney cells
HemA	Hemagglutinin A
HepG2	Hepatocellular carcinoma cells
HMGCoA	3-hydroxy-3-methylglutaryl coenzyme A
HNF1α	Hepatocyte nuclear factor - 1 alpha
HuH7	Human Hepatoma cells
IDL	Intermediate density lipoprotein
INSIG	insulin-induced gene 1

ITS	Insulin transferrin selenium
K_i	Inhibitor constant
LDL	Low density lipoprotein
LDL-C	Low density lipoprotein - cholesterol
LDLR	Low density lipoprotein receptor
LRP	LDLR-related protein
NARC-1	Neural apoptosis-regulated convertase - 1
PBS	Phosphate buffered saline
PBS-CM	Phosphate buffered saline with calcium and magensium
PC	Phosphatidylcholine
PCR	Polymerase chain reaction
PCs	Proprotein convertases
PCSK9	Proprotein Convertase Subtilisin / Kexin Type-9
PE	Phosphatidylethanolamine
RCT	Reverse cholesterol transport
RNA	Ribonucleic acid
S1P / S2P	Site - 1 Protease / Site - 2 Protease
SCAP	SREBP cleavage–activating protein
SDS-PAGE	Sodium dodecyl-sulfate - polyacrylamide gel electrophoresis
SEM	Standard error of the mean
SRE	Sterol regulatory element
SREBP	Sterol regulatory element binding protein
TAG	Triacylglycerol
TBSC	Tris-buffered saline with calcium
TFR	Transferrin receptor
UK	United Kingdom

List of Figures

1. Introduction

According to the Public Health Agency of Canada, one in three Canadians will die from cardiovascular disease (CVD), many under the age of 65[1]. It has become well known that CVD is the leading cause of death in the western world, and is also becoming an important cause of death in other parts of the world as various societies move towards affluence and industrialization[2]. Hypercholesterolemia, or elevated blood cholesterol levels, is the leading established causal factor associated with heart disease. Lowering blood cholesterol levels, in particular low-density lipoprotein (LDL) associated cholesterol levels, is the major form of therapy employed in CVD prevention and treatment. While statin drugs have long been the established and relatively successful method for lowering plasma LDL-cholesterol, adverse effects have been associated with their use, and patients do not always reach their target plasma LDL-levels[3].

A new class of cholesterol-lowering drugs have recently been in the making, revolving around the inhibition of the protein Proprotein Convertase Subtilisin / Kexin Type-9 (PCSK9). PCSK9 is a relatively recent discovery in the cholesterol metabolism field, acting as a negative regulator of LDL receptors (LDLRs) in the liver, impairing clearance of plasma LDL. The PCSK9 gene is now the third locus associated with autosomal dominant hypercholesterolemia (ADH), in addition to the genes for LDLR and Apolipoprotein B (ApoB)[4]. While a few monoclonal anti-PCSK9 antibodies have already made it to clinical trials[5], all aspects of PCSK9 biology have not yet been elucidated. One example is the very recently established interaction between PCSK9 and the LDL particles themselves, and the inhibitory effect that this has on the LDLR-degrading activity of PCSK9[6-8]. The project

described herein sought to investigate structural aspects of this interaction and how PCSK9 regulates circulating LDL-cholesterol levels.

1.1 Cholesterol

Cholesterol is a molecule of fundamental importance to both the structure and function of animal cells. Cholesterol can make up upto 50% molar proportion of the lipid content in cell membranes, regulating the fluidity and composition of the membranes[9]. It is an important component of lipid rafts and caveolae, and plays a role in cell signalling[10]. Furthermore, cholesterol is the structural basis of steroid hormones such as the sex hormones and glucocorticoids[9], and is an integral component of bile. But while cholesterol performs many essential functions, too much intracellular cholesterol is toxic to cells, and too much in the circulation can lead to deposits that form atherosclerotic plaques. Cholesterol synthesis or uptake from the circulation must therefore be balanced and well regulated.

1.1.1 Cholesterol synthesis

Cells obtain cholesterol through either extracellular or intracellular means. The intracellular pathway involves biosynthesis of cholesterol in the cell through the mevalonate pathway, while the extracellular pathway involves uptake of dietary cholesterol from the circulation. All cells produce cholesterol endogenously, although in hepatic tissue, much of the cellular cholesterol comes from the circulation. Intracellularly synthesized cholesterol derives all its carbons from acetate[9]. Acetyl-Coenzyme A (acetylCoA) is converted to 5-carbon isoprene units, which are then condensed into the linear precursor squalene. Squalene cyclizes to form lanosterol, which eventually leads to the formation of the 27-carbon cholesterol. The conversion of acetyl-CoA to isoprene units involves the intermediate 3-

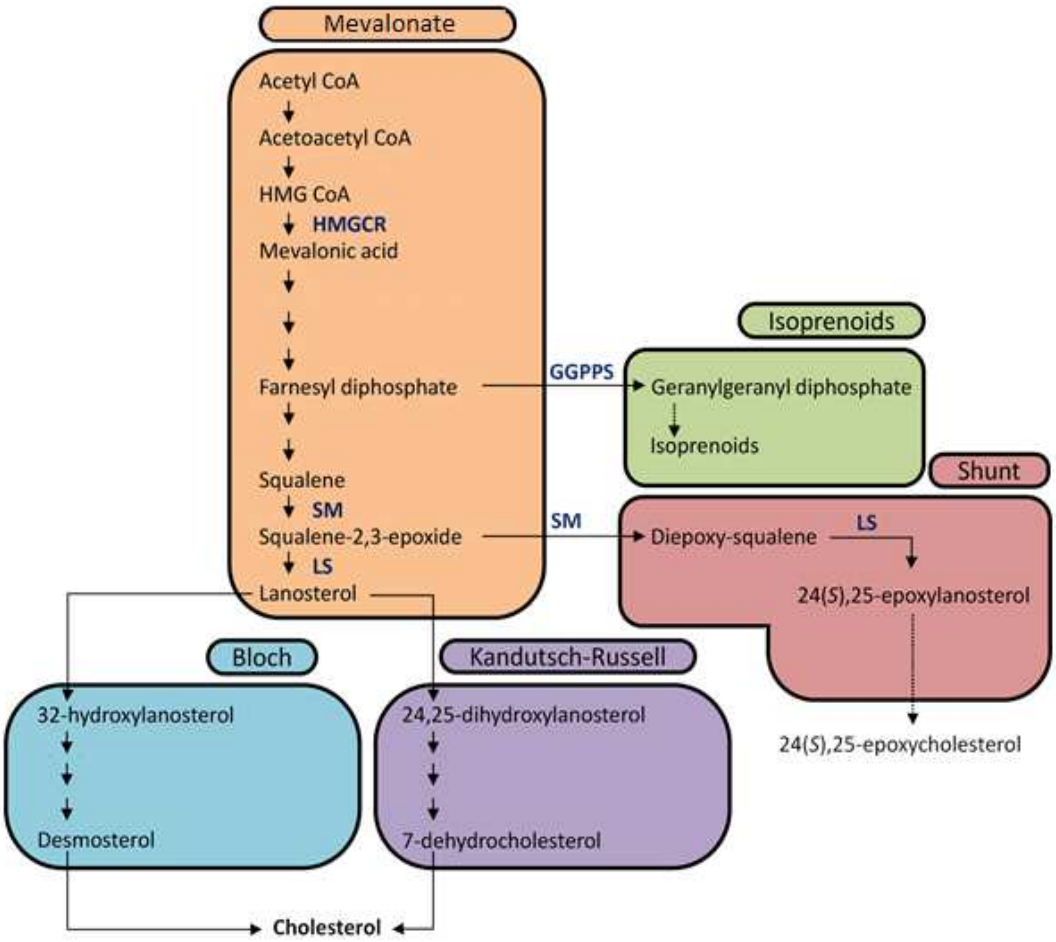

Figure 1: The intracellular cholesterol synthesis pathway. The mevalonate pathway contains the major rate limiting enzyme of the entire process, 3-hydroxy-3-methylglutaryl coenzyme A reductase (*HMGCR*). From lanosterol, cholesterol is formed after multi-step processes in the Bloch or Kandutsch pathways. Important branch points stem from flux of farnesyl diphosphate into the isoprenoids pathway, catalyzed by geranylgeranyl-diphosphate synthase(*GGPPS*), and from flux of squalene-2,3-epoxide into the Shunt pathway via squalene monooxegenase (*SM*) catalysis**.** Figure adapted from Sharpe et al, 2013[11].

hydroxy-3-methylglutaryl coenzyme A (HMGCoA), which is converted to mevalonate by the enzyme HMGCoA reductase (Figure 1). This enzyme catalyzes the rate limiting step and is the major flux control-point of the mevalonate pathway. It is regulated by negative feedback via intracellular cholesterol levels.[11]

The cholesterol synthesis pathway is large and complex, beginning in the cytosol or peroxisome and ending with the squalene-to-cholesterol conversion in the endoplasmic reticulum[9]. Many of the enzymes and intermediates involved are subject to feedback j produce metabolites important to other pathways, such as isoprenoids or epoxycholesterol (Figure 1). Sterol intermediates downstream of lanosterol are important for vitamin D production and meiosis activation[11]. While HMGCoA reductase is the rate-limiting reaction, it has also been suggested that squalene mono-oxygenase, the enzyme acting on squalene before cyclization, is another significant negative-feedback control point for the pathway, occurring late enough in the pathway to preserve flux into the isoprenoid branches[11, 12].

1.1.2 Cholesterol absorption, transport and plasma clearance

Lipoproteins. Cholesterol is transported in the circulation in macromolecular structures known as lipoproteins, along with fatty acids and triacylglycerol. Lipoproteins, as aggregates of proteins and lipids, facilitate transport of lipids in the aqueous environment of the circulation. The general structure of lipoproteins involves a phospholipid outer layer with the hydrophilic head groups on the exterior and the hydrocarbon tails facing a hydrophobic core. The phospholipid outer layer also contains free cholesterol, with the polar hydroxyl groups facing the exterior. The hydrophobic core carries fatty acids in the form of triacylglycerols (TAG), and cholesterol in the form of cholesterol esters (Figure 2B), along with fat-soluble

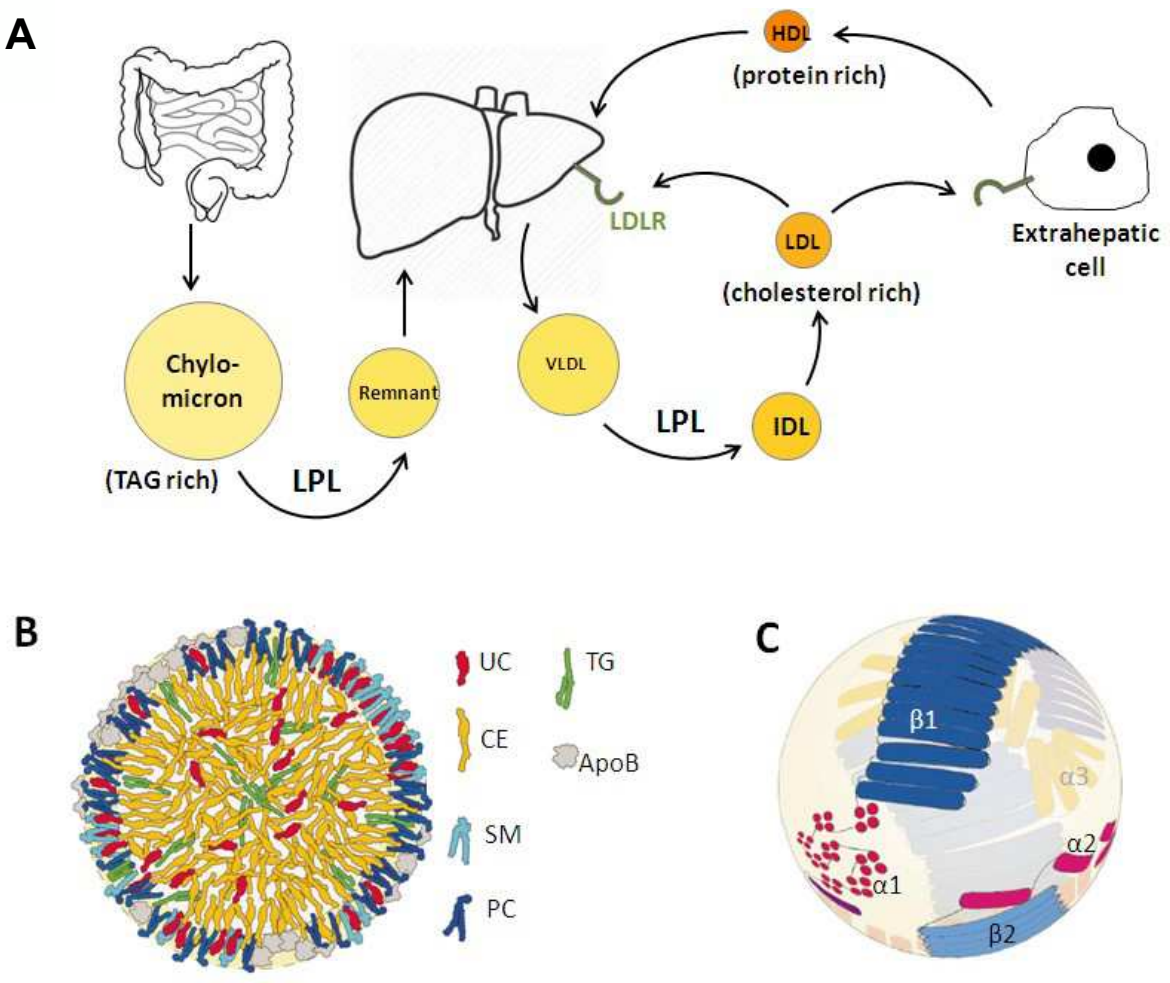

Figure 2: Cholesterol transport in circulation. (A) Circulation and metabolism of lipoproteins. Chylomicrons rich in dietary fat and cholesterol in the form of triacylglycerols (TAG) and cholesterol esters. Lipoprotein lipase- mediated catabolism in the circulation releases free fatty acids to peripheral tissues and forms chylomicron remnants which are taken up by the liver. The liver produces TAG-rich very low density lipoproteins (*VLDL*) which also get catabolised in the circulation by LPL to intermediate and low density lipoproteins (*IDL, LDL*). Cholesterol-rich LDL is cleared from the circulation by the liver through LDL receptor (*LDLR*) mediated endocytosis. Other tissues expressing LDLRs can also internalize LDL-cholesterol. High density lipoproteins (HDL) are also produced by the liver and are involved in carrying cholesterol from the periphery back to the liver. (**B) Cross section of an LDL particle showing general structure and composition.** The outer phospholipid layer consists primarily of phosphatidylcholine (PC) and sphingomyelin (SM), in addition to other kinds of phospholipids, with the very large Apolipoprotein B100 (ApoB) embedded around the surface. The hydrophobic core contains mainly esterified cholesterol (CE), with small amounts of unesterified cholesterol (UC) and triglycerides (TG). Some UC also found in the outer layer. (**C) A semitransparent representation of an LDL particle showing the different domains of ApoB around the particle**. Blue domains are beta sheets while pink or yellow domains contain alpha helices. Panels (B) and (C) adapted from Hevonoja, 2000[15].

vitamins[13]. Proteins termed apolipoproteins are embedded on the outer surface of the lipoproteins, and act as ligands for the respective cell-surface receptors for each class of lipoprotein. There are several classes of apolipoproteins, some of which can be exchanged between lipoprotein particles, and some of which cannot. There are also several types of lipoproteins, each with its own profile of apolipoproteins and lipid composition[13].

Lipids and cholesterol absorbed from food in the small intestine are first packaged into very large lipoproteins called chylomicrons containing apolipoprotein (apo) B48, which are heavily TAG-rich. Within hours, they are catabolised in the circulation by the enzyme lipoprotein lipase (LPL) into chylomicron remnant particles, releasing fatty acids for utilization in peripheral tissue. The chylomicron remnants, now considerably richer in cholesterol esters, acquire Apolipoprotein E in the circulation and are taken up by endocytosis in the liver through binding to cell surface lipoprotein receptors, including LDLR and LDLR-related protein (LRP). The liver produces TAG-rich very low-density lipoproteins (VLDL) containing apoB100, which are also catabolised in the circulation by LPL to the short lived intermediate-density lipoprotein (IDL) and finally to LDL, again releasing fatty acids to peripheral tissues in the process. The liver then clears both LDL from the plasma via an interaction between LDLR and its ligand apoB100. High-density lipoproteins (HDL) are also produced by the liver in the form of lipid-poor ApoA-I[9, 13]. These are the smallest, densest lipoproteins, being protein-rich, and are involved in the athero-protective process of reverse cholesterol transport (RCT). Excess cholesterol from peripheral cells and vessel walls is effluxed back to the liver through the RCT pathway. Poorly lipidated HDL particles act as cholesterol acceptors from the peripheral cells and carry the cholesterol to the liver for excretion through bile[14] (Figure 2A).

LDL. LDL is a relatively small, dense, cholesterol-rich lipoprotein, on average about 22nm across and generally in the density range of 1.019-1.063 g/ml[15]. Within each class of lipoprotein there exists considerable heterogeneity in terms of size, density and composition, and this holds true for LDL as well. LDL exists in subclasses ranging from large buoyant (over 26nm diameter, density 1.025-1.035 g/ml) to progressively smaller, denser LDL, with the latter subtype having a higher association with atherosclerosis and myocardial infarction[16-18]. LDL is the main carrier of plasma cholesterol, and its cellular uptake via the LDLR is the primary means of plasma cholesterol clearance in humans. The liver is the main organ responsible for plasma LDL clearance[13].

The phospholipid component of LDL is primarily phosphatidylcholine (PC) and sphingomyelin, followed by lyso-PC and phosphatidylethanolamine (PE), in addition to others[15] (Figure 2B). Each LDL particle contains one non-exchangeable apoB100 molecule as its only apolipoprotein moiety, acting as the ligand for the LDLR[15, 19]. ApoB is one of the largest known proteins (4536 residues) and is insoluble, making structural studies of ApoB difficult. However, electron microscopy revealed that ApoB is wrapped around the LDL particle in a three-dimensional conformation containing kinks [15]. Circular dichroism indicated the presence of alpha helices and beta sheets. Computational analyses led to the picture of a penta-partite model of the ApoB100 protein, with three regions of amphipathic alpha helices alternated by two regions of amphipathic beta sheets (Figure 2C). It is the continuous amphipathic beta sheet regions that are believed to confer the high lipid-affinity and non-exchangeability of the ApoB100 on LDL[20, 21].

LDLR. The LDLR is a modular, transmembrane, calcium-dependent receptor 839 residues long. The extracellular N-terminal region contains a ligand-binding domain with seven

cysteine-rich repeats, in which lies the ApoB binding site that allows binding to LDL as well as other ApoB containing lipoproteins, VLDL and chylomicron remnants. Apolipoprotein E, found on chylomicrons, VLDL, IDL and HDL, is also a ligand for the LDLR[13]. This is followed by epidermal-growth-factor-like domains A and B (EGF-A and EGF-B), a β-propeller domain, an EGF-C domain, a section of O-linked glycans, a transmembrane domain, and finally a short, intracellular C-terminal tail required for endocytosis of the protein, in conjunction with the adaptor protein ARH (autosomal-recessive hypercholesterolemia)[22-24]. The EGF-A domain is the binding site of PCSK9 on LDLR[25]. Each LDLR binds one ApoB100 moiety at a time, and the LDLR-LDL complexes formed in cell-surface clathrin-coated pits are endocytosed[26]. In the low-pH and low-calcium environment of the endosomes, the LDLR adopts a "closed" conformation, releasing the lipoprotein. The LDL migrates to the lysosome for further catabolism, while the receptors are recycled back to the cell surface to continue lipoprotein uptake into the cell[27]. The recycling period for an LDLR is about 10min, with a total lifespan of about 20hrs[28].

1.1.3 Transcriptional regulation of cholesterol pathways

A large number of genes in the lipid and cholesterol synthesis pathways in humans contain sterol regulatory elements (SREs) in their promoters. These genes are regulated by the sterol regulatory element binding protein (SREBP) transcription factors. Of the three SREBP isoforms, SREBP-1a plays a broad role in regulating all SREBP-responsive genes, while SREBP-1c is more limited to regulating the fatty-acid synthesis pathway. The third isoform, SREBP-2, is the transcription factor that preferentially governs the cholesterol synthesis and uptake pathways. Overexpression of truncated SREBP-2 that is non-susceptible to negative

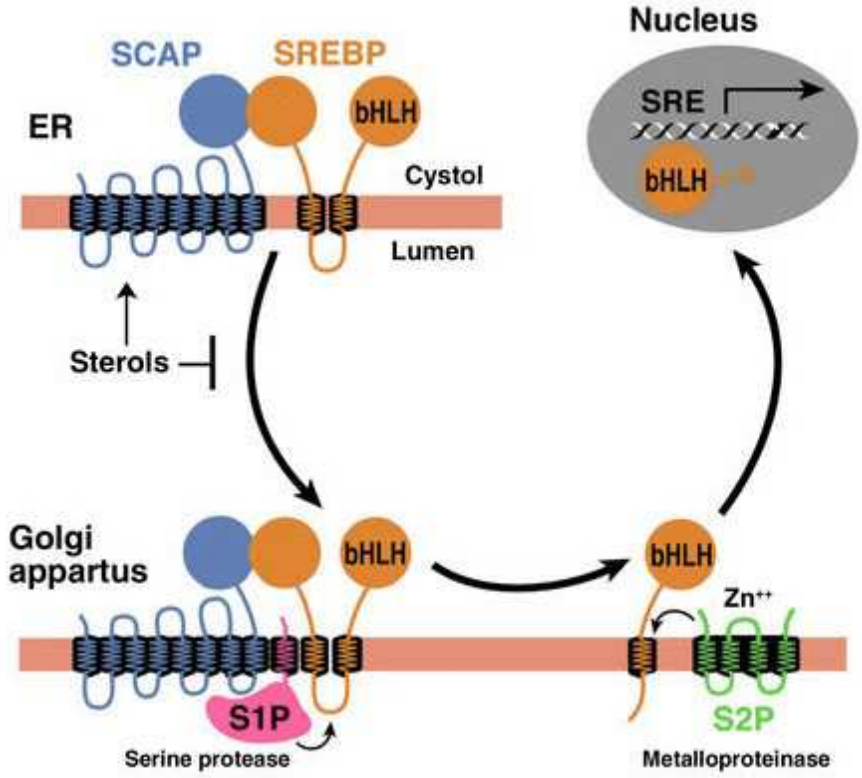

Figure 3: Transcriptional regulation of the cholesterol synthesis pathway by SREBP-2. SREBP-2 remains anchored at the endoplasmic reticulum (ER) membrane bound to SREBP cleavage–activating protein (SCAP). SCAP is a sterol sensing protein. At low cellular cholesterol levels, SCAP escorts SREBP-2 to the Golgi, where cleavage by site-1 protease (S1P) and site-2 protease (S2P) cause release of the N-terminal of SREBP-2, which can then travel to the nucleus as an activated transcription factor and upregulate genes in the intracellular cholesterol synthesis pathway and related targets. Figure taken from Horton, Goldstein and Brown, 2002.

regulation by cholesterol in transgenic mice showed an increase in mRNA of numerous cholesterol synthesis and uptake pathway genes, including HMGCoA reductase, LDLR and PCSK9[29].

SREBP-2, like the other two SREBPs, is a basic helix-loop-helix transcription factor that is synthesized as an inactive precursor. To be activated, the N-terminal domain must be released by cleavage so it can move to the nucleus. Inactive SREBP-2 is bound to the endoplasmic reticulum (ER) membrane, with the C-terminal bound to the escort protein SREBP cleavage–activating protein (SCAP). SCAP is a sterol sensor which, at high cholesterol levels, is bound to the ER anchor protein insulin-induced gene 1 (INSIG-1), retaining SREBP-2 at the ER with it. However, at low cholesterol levels, SCAP undergoes a conformational change[30] allowing it to dissociate from INSIG-1 and escort SREBP-2 to the Golgi. In the Golgi are two proteases: site-1 protease (S1P) and site-2 protease (S2P), which cleave SREBP-2, releasing the active N-terminal of SREBP-2[10] (Figure 3).

In addition to the post-translational regulation of SREBP-2 activity by sterol levels, SREBP-2 also regulates its own transcription in a positive-feedback mechanism through an SRE motif present in its own promoter[31].

1.1.4 Cholesterol in disease

Hypercholesterolemia and atherosclerosis. Modern diet and lifestyle, in combination with genetic risk factors, have led to widespread hyperlipidemia and high blood cholesterol levels, which in turn can lead to diseases such as atherosclerosis and coronary heart disease (CHD), the major causes of morbidity and death in the West. Multiple epidemiological studies have linked high blood cholesterol levels with CHD[32]. LDL carries the majority of the cholesterol

content in the blood, and elevated plasma LDL levels are the major causative risk factor for CHD. Below 100mg/dL of LDL-cholesterol is considered optimal for health, while over 160mg/dL LDL cholesterol is considered a high risk for disease[32].

Atherosclerosis develops when hypercholesterolemia, or chronic high levels of LDL in the circulation, leads to entry and retention of LDL particles in artery walls[33-35]. Retained lipoproteins undergo modifications within the endothelium, such as oxidation and aggregation[35]. This leads to a cascade of inflammatory responses and formation of atherosclerotic plaques, which impede blood flow. Cholesterol-loaded foam cells, lipid droplets and cholesterol crystals make up necrotic cores in plaques[36]. Fibrous caps form around these plaques. Breaks in the fibrous caps can lead to formation of a thrombus, further blocking blood flow and potentially leading to a heart attack or heart failure. The thrombus can also detach and travel in the circulation, potentially lodging elsewhere in the body, leading to complications such as stroke or ischemia[36].

Autosomal dominant hypercholesterolemia (ADH) is a hereditary form of hypercholesterolemia arising primarily from mutations in the genes for ApoB or LDLR, and more rarely from gain-of-function mutations in PCSK9, disrupting plasma LDL clearance and leading to greatly increased risks for CHD[37, 38].

Statins. Statins are HMGCoA reductase inhibitors, and are the major class of drugs used to treat hypercholesterolemia. By blocking the rate-limiting step in cholesterol synthesis, statins induce cells to upregulate expression of the LDLR and increase plasma LDL clearance. Statins are a very widely prescribed and successful class of drug, reaching 18-55% reductions

in LDL cholesterol levels[32]. However, as noted previously, the HMGCoA reductase reaction occurs upstream of important branch points in the mevalonate pathway that produce isoprenoid intermediates for end products such as Hem A and ubiquinone (for the electron transport chain), dolichol (for glycoprotein synthesis), isopentyladenine (for transfer RNAs) and farnesylation of proteins[39, 40] . Adverse effects have been associated with statin use, primarily myopathies such as myositis and rhabdomyolysis. Many of the adverse effects are related to stresses on mitochondrial function, likely stemming from interference in cellular production of ubiquinone and Hem A[41, 42].

1.2 PCSK9

In 2003, Seidah *et al* characterized a new secretory mammalian proprotein convertase named neural apoptosis-regulated convertase 1 (NARC-1), later known as PCSK9, or proprotein convertase subtilisin/kexin type-9[43]. It was highly expressed in the liver, and at lower levels in a limited number of other tissues including the kidneys and intestines. In the same year, Abifadel *et al* identified mutations in the PCSK9 gene as causing autosomal dominant hypercholesterolemia[4]. *PCSK9* thus became the third locus causally associated with ADH. In the decade since, PCSK9 has emerged as a potent regulator of blood LDL cholesterol levels and has become a target of great interest for hypercholesterolemia therapeutics. It has instigated a flurry of research and drug company activity and promises to give rise to a whole new class of cholesterol lowering drugs.

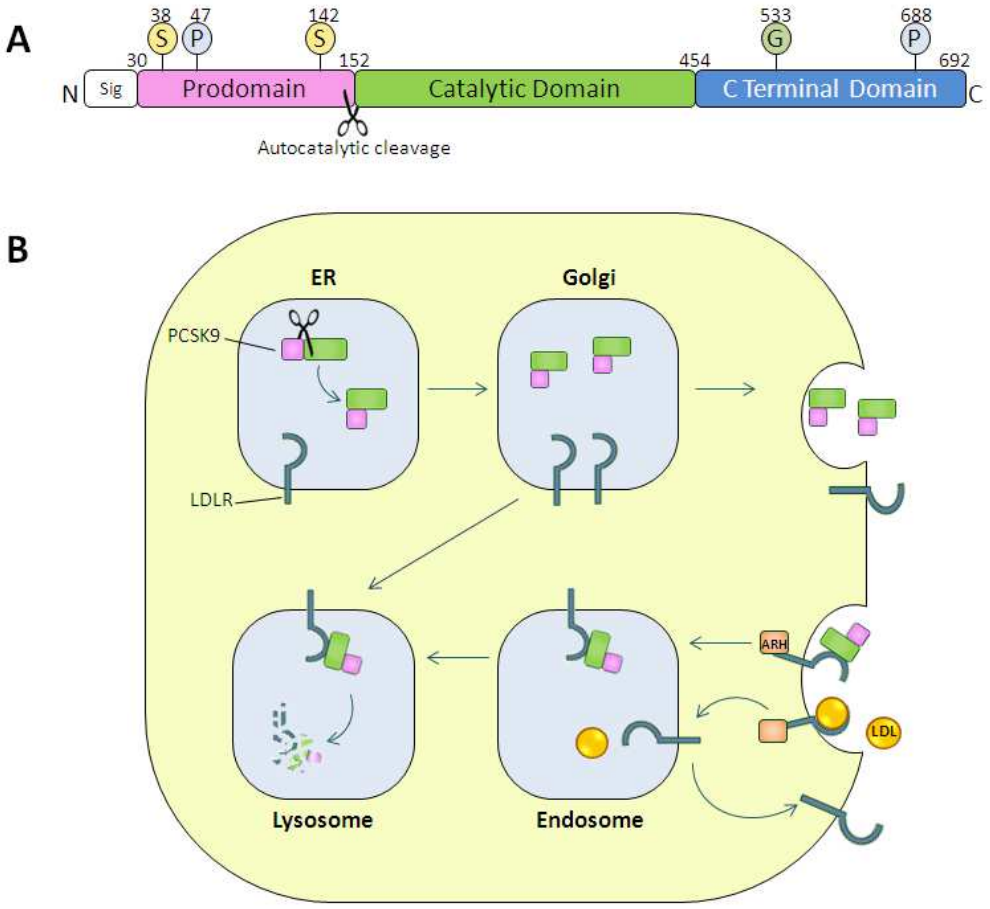

Figure 4: PCSK9 structure and cellular trafficking. (A) Schematic of pro-PCSK9, beginning with a signal sequence for secretion, followed by the prodomain, catalytic domain and C-terminal domain. Autocatalytic cleavage occurs between residues Q_{152} and S_{153}, removing the prodomain, which remains associated with the rest of the mature protein. Post-translational modification sites exist on the protein at tyrosine 38, serine 47, tyrosine 142, asparagine 533, and serine 688. S: sulfation, P: phosphorylation, G: N-linked glycosylation. **(B) PCSK9 secretion and LDLR degradation.** Pro-PCSK9 is self-processed in the endoplasmic reticulum (ER), exported to the Golgi, and secreted into the circulation. LDLR at the cell surface can bind low density lipoproteins (LDL), in which case, after endocytosis, the complex dissociates and LDLR recycles back to the cell surface. Cell-surface LDLR can also bind circulating PCSK9. Once this complex is endocytosed, LDLR is directed to the lysosome for degradation, instead of recycling back to the cell surface.

1.2.1 PCSK9 Structure and cellular trafficking

Serine proteases are a large and diverse group of enzymes in the body that cleave proteins at particular peptide bonds through an active site with a catalytic triad made up of a serine histidine and aspartate. Serine proteases can be divided into two subfamilies that are either related to trypsin / chymotrypsin, or to bacterial subtilisin. Proprotein convertases (PCs) are a subtilisin-related family of serine proteases. Members of the PC family play roles in the processing and maturation of multiple precursor proteins at various locations in the cell, with most PCs cleaving after basic residues[44, 45].

PCSK9 is the ninth member of the PC family, synthesized in the endoplasmic reticulum (ER) as a 692 amino acid zymogen. Similar to other PC members, the PCSK9 zymogen has an N-terminal signal peptide followed by three domains: the prodomain, the catalytic domain and a cysteine and histidine-rich C terminal domain (Figure 4A). Typically, PCs undergo cleavage and release of the prodomain in the ER, with the exception of PC2. PCSK9 cleaves after non-basic residues[46], and performs its own prodomain cleavage between Q_{152} and S_{153}. As with other PCs, the PCSK9 prodomain remains associated non-covalently with the catalytic domain to form the mature zymogen. In other PCs, a secondary cleavage event releases the inhibitory prodomain, resulting in an active enzyme. However, the C-terminal end of the associated prodomain in PCSK9 remains tightly bound in the catalytic site and blocks the catalytic triad (Asp186, His226 and Ser386) from binding any substrate, preventing mature PCSK9 from acting as a serine protease. No substrates of PCSK9 other than itself have yet been identified[46].

Crystal structures of PCSK9 do not show the N-terminal of the prodomain up until residue 60, indicating that the region is structurally disordered[46-48] (Figure 5A). The remainder of the

prodomain is made up of a 5-stranded β-sheet covered on one side by two alpha helices. Residues 61-75 form an extra strand, deemed to be important for self-processing, followed by a helical turn. The strand and turn enlarge the interface of the PCSK9 prodomain with the catalytic domain, contributing to retention of the prodomain on the mature protein in contrast to the other PCs[46]. The catalytic domain contains a 7-stranded parallel β-sheet flanked on both sides by alpha helices. The domain contains three disulfide bonds, with two alpha helices forming the interface with the C-terminal domain. The C-terminal domain has a cylindrical overall structure made up of three subunits with quasi-three fold internal symmetry. Each subunit is made up of 6-stranded anti-parallel β-sheets in truncated jelly-roll motifs; the subunits are held together by three internal disulfide bonds each[47, 48]. The catalytic domain is attached to the C-terminal domain by three hydrogen bonds, with the remaining interaction being hydrophobic or Van der Waals forces. The C-terminal domain also contains a high number of histidine residues, mostly concentrated on the surface of a groove between two of the subunits[47].

The prodomain of PCSK9 acts as a chaperone for normal folding and secretion[49]. Translated PCSK9 is exported as soluble cargo from the ER to the Golgi in coat protein complex II (COPII) coated vesicles in a SEC24-dependent manner[50]. PCSK9 also undergoes several post-translational modifications in the ER and Golgi. An N-linked glycosylation site exists at N533[43], as well as two sulfation sites at Tyr38 and Tyr142[43, 51] and a phosphorylation site at Ser47[52]. The functional purposes of these post-translational modifications have yet to be elucidated. Fully matured PCSK9 is then secreted into the circulation, primarily from hepatocytes. PCSK9 is also expressed at lower levels in the kidneys, cerebellum and small intestine[43] .

1.2.2 PCSK9 in LDLR degradation

PCSK9 is a unique member of its family in its inability to function as a serine protease in mature form. Secreted PCSK9 in the circulation does however, perform a very significant form of blood cholesterol regulation through its ability to bind LDLRs at the cell surface and target them for degradation in the lysosome upon endocytic internalization. This disrupts the recycling of the LDLR and decreases LDLRs expressed at the cell surface, thus decreasing plasma LDL clearance. In cell culture, adenoviral overexpression of PCSK9 in hepatocyte cell lines corresponded with a large reduction in LDLR expression[53]. *In vivo*, injection of PCSK9-expressing adenovirus in wild-type mice also led to a reduction in liver LDLR and corresponding increases in plasma LDL-cholesterol[53,54]. Parabiosis experiments demonstrated that human PCSK9 in the circulation of transgenic mice was able to decrease hepatic LDLRs in wild-type mice through shared circulation[55].

PCSK9 binds the EGF-A domain of the LDLR in a 1:1 ratio and a calcium dependent manner[46]. Crystal structures show PCSK9 bound to the EGF-A domain through a site on its catalytic domain (Figure 5B), primarily by hydrophobic interactions as well as a number of salt bridges and hydrogen bonds which contribute to specificity[25]. Mouse and cell culture studies where gain-of-function PCSK9 mutant D374Y caused greater PCSK9 uptake and hepatic LDLR degradation support the specificity of the LDLR-PCSK9 interaction[56]. The affinity of PCSK9 for the LDLR EGF-A domain increases at endosomal pH, and increased overall affinity to LDLR at acidic pH may involve further contacts between the LDLR ligand binding domain and the prodomain and C-terminal domains of PCSK9[37].

The C-terminal domain of PCSK9 has been shown to be required for LDLR degradation activity, although it remains unknown whether this is through a structural role or through

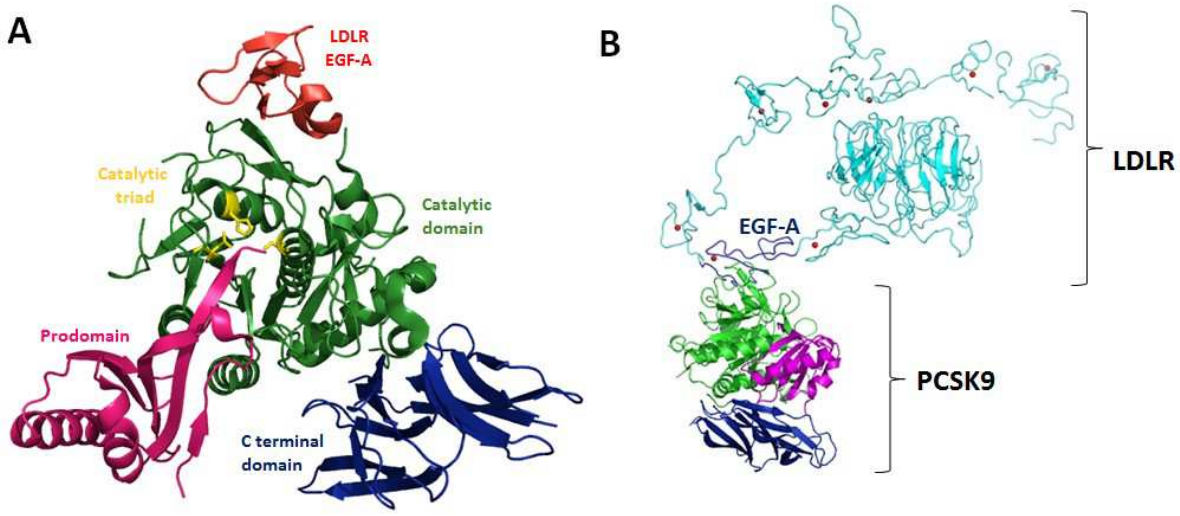

Figure 5: Crystal structure of PCSK9. (A) The three domains of PCSK9 are shown in pink (prodomain), green (catalytic domain) and blue (C terminal domain). The LDLR EGF-A (red) binding site is on the surface of the catalytic domain. The C-terminal end of the cleaved prodomain blocks the catalytic triad (yellow stick residues) and prevents the protease activity of mature PCSK9. Neither the N-terminal of the prodomain or the third subdomain of the C-terminal domain are visible in this structure. Panel adapted from RCSB Protein Data Bank structure 3BPS, modified on Pymol software. (**B) Crystal structure of PCSK9 bound to LDLR at acidic pH.** PCSK9 binds the LDLR at the EGF-A domain, through a site on its catalytic domain. The EGF-A domain is shown in dark blue while the rest of the receptor is in light blue. Red spheres indicate calcium ions. Figure adapted from Kwon *et al*, 2008[25].

binding to LDLR or another protein co-factor [57]. The precise mechanism of PCSK9-mediated LDLR degradation remains undetermined. Mature PCSK9 does not act as a serine protease. Thus its LDLR-degrading activity is not through a catalytic mechanism. A catalytically dead PCSK9 mutant (S386A) was expressed in HepG2 cells in trans with its prodomain in order to bypass the need for self-processing for secretion. This PCSK9 variant was comparable to wild-type in its ability to direct LDLR degradation[58]. In vitro studies support that PCSK9 may lock internalized LDLR in an open conformation, preventing recycling and targeting the receptor for lysosomal degradation[37, 59]. An N-terminal region of the prodomain is auto-inhibitory to the ability of PCSK9 to bind and degrade LDLRs. Removal of residues 31-52 led to an increased affinity of PCSK9 for the extracellular domain of the LDLR in vitro [25]. Furthermore, removal of a stretch of acidic residues within this N-terminal region (residues 33-40) appeared to increase cell-surface LDLR degradation by 31%, as indirectly assessed through LDL uptake in HepG2 cells[60].

Interestingly, PCSK9 exhibits tissue-specific activity, preferentially degrading hepatic cell-surface LDLRs over LDLRs on non-hepatic cells[53, 56, 61, 62]. Annexin A2 has been suggested as a natural extra-hepatic inhibitor of PCSK9[62]. More recently, Nguyen *et al* found that in SV-589 fibroblasts, exogenous wild-type PCSK9 readily dissociates from LDLR in early endosomes to be degraded in the lysosome, in contrast to gain-of-function D374Y-PCSK9 which continues to recycle back to the cell-surface, presumably still bound to LDLR. Unlike wild-type PCSK9, the D374Y-PCSK9 was able to achieve limited LDLR degradation in the fibroblast cells at high, non-physiological concentrations. This suggests that an increased endosomal dissociation of PCSK9 from LDLR in non-hepatic cells may play a role in tissue specificity as well[61].

While PCSK9 acts as a potent regulator of hepatic LDLR levels, circulating PCSK9 levels are also reciprocally regulated by the LDLR. Acute overexpression of human LDLR in mice was capable of reducing plasma PCSK9 by 67%, injected PCSK9 showed delayed clearance from plasma in LDLR knockout mice, and injected LDL clearance patterns were similar to PCSK9 clearance patterns[8, 56]. Furthermore, increased plasma clearance of gain-of-function mutant PCSK9-D374Y compared to wild-type PCSK9 directly implicates the PCSK9 interaction with the LDLR EGF-A domain as an important regulator of circulating PCSK9 levels[56].

1.2.3 Transcriptional regulation of PCSK9

PCSK9, like many of the cholesterol synthesis and regulation-related genes, is transcriptionally regulated by the SREBP-2 transcription factor through a SRE on its proximal promoter. This creates an interesting situation where SREBP-2 mediated activation simultaneously increases cellular LDLR levels and upregulates PCSK9 secretion, which then leads to degradation of the LDLRs. This problem is also a feature of statin treatment, as the SREBP-2 mediated upregulation of LDLRs in response to HMGCoA inhibition also leads to PCSK9 upregulation[63].

The PCSK9 promoter also contains a functional binding site for the transcription factor HNF1α shortly upstream of the SRE[64]. HNF1α appears to work in concert with SREBP-2 in the activation of PCSK9 transcription. HNF1α is a liver-enriched transcription factor, regulating genes in the liver and intestines, which may help to explain the high expression of PCSK9 in the liver[64]. HNF1α gene targets are also involved in lipid and cholesterol metabolism, as well as acute-phase inflammatory responses, thus possibly forming a connection between PCSK9 and inflammation[65].

1.2.4 Closing the triangle: PCSK9 and LDL

The project described herein revolves around the very recently observed interaction between PCSK9 and LDL particles[6-8]. Over 30% of plasma PCSK9 in normolipidemic subjects has been observed bound to LDL[8]. In vitro studies using IR-dye labelled PCSK9 show that the interaction can be competed by unlabelled PCSK9 and fits a one-site binding model[6]. Data on the interaction is consistent with a protein-protein interaction between PCSK9 and the ApoB100 moiety on LDL[7]. PCSK9 appears not to bind to VLDL despite the presence of ApoB on VLDL particles[6]. This may be due to the PCSK9 binding site on ApoB only becoming available after lipoprotein remodeling by either lipoprotein lipase during conversion of VLDL to IDL and LDL, or by the enzyme cholesteryl ester transfer protein (CETP), which exchanges triglycerides from ApoB-carrying lipoproteins with cholesteryl esters from HDL[65]. Deletion of the N-terminal region of the PCSK9 prodomain (residues 31-52) results in loss of LDL-binding, implicating this region on PCSK9 as either the physical LDL-binding site or an important regulator of the interaction[6]. It interesting to note that this is the same N-terminal region that is auto-inhibitory to the LDLR-degrading activity of PCSK9.

Importantly, PCSK9 also shows decreased LDLR-degrading activity in the presence of LDL. The LDLR-binding site on the catalytic domain of PCSK9 does not overlap with the LDL-binding site, as demonstrated in vitro by agarose gel mobility shift assays[6]. This indicates that the inhibition of PCSK9 binding to LDLR by LDL does not occur through a competitive mechanism. The actual mechanism of inhibition remains unknown.

1.2.5 PCSK9 as a therapeutic target

The existence of loss-of-function PCSK9 variants in healthy humans pointed to the possibility of PCSK9 inhibition as a viable therapeutic approach to treat hypercholesterolemia. The nonsense mutations Y142X, C679X, frequently found as heterozygotes in African American populations, have been linked to 30%–40% reductions of plasma LDL-cholesterol and over 80% reductions in CVD risk[66, 67]. In fact, two individual women were identified to be lacking circulating PCSK9 altogether. Both of these women had less than 15mg/dL plasma LDL-cholesterol, and neither showed any adverse effects on their health due to the lack of functional PCSK9[68, 69].

PCSK9 inhibition would be useful either on its own or in conjunction with statin treatment. Since statin treatment simultaneously increases expression of both LDLR and PCSK9 through SREBP2 activation, PCSK9 inhibition would have the benefit of further increasing the efficiency of the statin treatment. Inhibition of PCSK9 has been investigated along several avenues, including gene silencing through antisense oligonucleotides or RNA interference, and mimteic peptides or monoclonal antibodies that aim to disrupt the PCSK9-LDLR interaction[5, 37]. Monoclonal antibodies have been the most promising so far, with several large pharmaceutical companies developing antibodies that have advanced to clinical trials. Notably, the antibodies AMG145 and REGN727/SAR23655 reached 3rd phase clinical trials and have demonstrated LDL-cholesterol reductions approaching 80%[5]. However, while antibodies look promising, there remains interest in developing small-molecule inhibitors of PCSK9 function that are less costly and have better tissue-distribution.

1.3 Research rationale and objectives

The importance of the N-terminal region of the PCSK9 prodomain in both LDL binding and in auto-inhibition raise the possibility that this region is involved in an allosteric mechanism that regulates PCSK9 function. The inhibition of PCSK9 in the presence of LDL suggests that LDL-association may stabilize PCSK9 in an auto-inhibited conformation. LDL-bound PCSK9 in the circulation could thus potentially form pools of inactive PCSK9 in equilibrium with active non-LDL bound PCSK9 contributing to overall blood cholesterol homeostasis.

While the amino acid 31-52 region of PCSK9 has been shown to be required for LDL binding[6], it remains unclear whether the binding site of PCSK9 does in fact lie in this region or whether it is a conformational modulator of the interaction. Which specific residues within this disordered region are required for the LDL interaction is also unknown. Thus, the first objective of this project was to map the N-terminal region for specific residues required for LDL-binding using site-directed mutagenesis.

Based on the finding that LDL-association negatively regulates PCSK9 function, we also hypothesized that PCSK9 variants defective in LDL-binding would remain unaffected in their ability to bind LDLR in the presence of LDL. Thus, the second objective of the project was to test this hypothesis in cell culture by evaluating the ability of PCSK9 prodomain mutants defective in LDL-binding to bind LDLRs.

2. Materials and Methods

2.1 Materials

2.1.1 Vectors

The pcDNA3.1-PCSK9-FLAG vector codes for full length human wild type PCSK9 with a FLAG-tag epitope attached at the C-terminus (From Dr. Jay Horton, University of Texas Southwestern Medical Center, Dallas). This vector was used as the template to generate PCSK9 mutants. LDLR cDNA expression vectors were pLDLR17[70] coding for human wild-type LDLR and the mutant LDLR-ΔR6 (Δ211–251, deletion of repeat 6 of the ligand binding domain) constructed in pLDLR17 (provided by R. Milne, University of Ottawa Heart Institute).

2.1.2 Chemicals and reagents

Phusion High Fidelity Polymerase and DpnI enzyme were from NEB, while dNTP mix was from Promega. One Shot Top Ten Chemically Competent E. coli, Lipofectamine 2000, Dulbecco's Modified Eagle's Medium (DMEM), Fetal Bovine Serum (FBS), 100X Sodium Pyruvate (100mM), Penicillin and Streptomycin sulfate were all obtained from Invitrogen. EDTA-free Complete™ Protease Inhibitor Tablets were from Roche Applied Science. Optiprep density gradient medium (60% w/v iodixanol) was obtained from Axis-Shield. Sulfo-NHS-SS-Biotin, Dylight 800 antibody labelling kits and Neutravidin Plus agarose bead slurry were from Thermo Scientific. 1,2-dioleoyl-sn-glycero-3-phosphocholine (DOPC) and 1,2-dioleoyl-sn-glycero-3-phosphoethanolamine (DOPE) were from Avanti Polar Lipids. All other reagents were obtained from Sigma unless otherwise stated.

2.1.3 Antibodies

Mouse anti-human transferrin receptor antibody (mbv) was purchased from Life Technologies. Biotin-labeled monoclonal anti-human IgG1 antibody, monoclonal anti-actin antibody (AC-10) and monoclonal anti-FLAG M2 antibody were from Sigma-Aldrich. Rabbit anti-serum 3143 against the C-terminal of LDLR was a gift from Joachim Herz, while 13D3, a monoclonal antibody against the catalytic domain of full length PCSK9, was a gift from J. Horton, both at the University of Texas Southwestern Medical Center, Dallas, TX. Secondary IRDye-labeled goat anti-mouse and anti-rabbit IgG antibodies were purchased from LI-COR Biosciences. The monoclonal antibodies 15A6 & 13D3 recognize the C-terminal domain and the catalytic domain of PCSK9 respectively[55], and are purified from hybridomas in the lab.

2.1.4 Media

Medium A: DMEM (4.5 g/L or 1g/L glucose; Invitrogen) supplemented with 100 units/ml penicillin and 100 μg/ml streptomycin sulfate.

Medium B: Medium A supplemented with 10% FBS

Medium C (serum-free medium): Medium A supplemented with 1X Insulin Transferrin Selenium (ITS) (Sigma)

Medium D (sterol depleting medium): Medium A supplemented with 5% (v/v) newborn calf lipoprotein-deficient serum, 10 μM pravastatin, and 50 μM sodium mevalonate.

Medium E (sterol supplemented medium): Medium A supplemented with 5% (v/v) newborn calf lipoprotein-deficient serum, 10 μg/ml cholesterol, and 1 μg/ml 25-hydroxycholesterol.

Medium F (PCSK9 treatment medium): Medium A supplemented with 5% (v/v) newborn calf lipoprotein-deficient serum and 1% (w/v) bovine serum albumin.

2.2 Methods

2.2.1 Mutagenesis of PCSK9

A modified version of the QuickChange™ site-directed mutagenesis protocol (Stratagene, La Jolla, CA) was used to introduce point mutations or deletions into wild-type PCSK9-FLAG. Forward and reverse primers, both of which carried the desired mutations, were designed according to QuickChange™ guidelines. 50 µl PCR reactions were carried out. Each reaction contained 1X phusion High Fidelity Buffer, 0.3 mM dNTP mix, 0.3 µM each of both forward and reverse primer, 1 ng/µl of template DNA and 1 unit of Phusion DNA polymerase. Thermocycling was initiated at 98°C for 30 seconds, followed by 25 cycles of amplification. Each cycle consisted of 10 seconds denaturation at 98°C, 30 seconds annealing at 62°C, and 30 seconds / kb of extension at 72°C. A final extension step of 10 minutes at 72°C concluded the reaction. PCR was followed by digestion of original non-mutant template strands with 10 units DpnI enzyme. 4 µl of the DNA was then transformed into One Shot Top Ten Chemically Competent E. coli. Bacterial transformant selection was done by plating on Luria Broth (LB) agar plates with ampicillin. Correctly mutated constructs were confirmed by sequencing.

2.2.2 Cell culture

All cells were maintained in monolayer cultures at 5% carbon dioxide and 37°C. HEK293 cells were maintained in Medium B containing 4.5 g/L glucose, while HepG2 cells were maintained in Medium B containing 1 g/L glucose.

2.2.3 PCSK9 Protein production

Conditioned media. HEK293 cells were grown in Medium B to ~80% confluency (see 2.2.5 Cell Culture) and then transiently transfected with 4 μg of DNA (either wild-type or mutant PCSK9-FLAG construct) and 12 μg Lipofectamine 2000 per 10 cm dish, according to Lipofectamine manufacturer instructions. Cells were put in serum free conditions (Medium C) the day after transfection and allowed to secrete PCSK9 for 48 hours before collecting the medium (centrifuged at 1000xg for 5min and filtered through 0.22 μm PVDF to remove cells). Medium was buffer exchanged with HBSC (HEPES Buffered Saline-Calcium buffer: 25 mM HEPES-KOH, pH 7.4, 150 mM NaCl, 2mM $CaCl_2$) and concentrated 20-fold in Amicon filters (10 kDa molecular weight cut-off, Millipore). PCSK9 concentration and quality was estimated and monitored through comparison to purified protein standards on SDS-PAGE and western blotting.

Purified Protein. Stably transfected HEK293 suspension cell lines expressing wild-type or mutant PCSK9 were seeded in 1L liquid cultures at 100,000 cells/ml in UltraDOMA™ hybridoma serum-free growth medium (Lonza) supplemented with 10% (v/v) FBS, 10mM L-Glutamine, 100 units/ml penicillin and 100 μg/ml streptomycin sulfate. Cultures were grown without carbon dioxide at 37°C with stirring at 93 rpm for 7 days. Medium was harvested by pelleting cells at 3700 rpm for 20 minutes and filtering through 0.22 μm Millipore filter units. The pH of the medium was adjusted by addition of 50 mM final concentration Tris-HCL at pH 7 (pH 7.4 at 4°C). FLAG-tagged protein was bound to anti-FLAG M2 affinity columns by gravity flow, washed in TBSC (Tris Buffered Saline-Calcium buffer: 50 mM Tris-HCl pH 7.4, 150 mM NaCl, 2 mM $CaCl_2$) and eluted with 100 μg/ml FLAG peptide (Thermo Scientific). The eluted protein was then concentrated 80-fold in

Amicon filter units (10 kDa molecular weight cut-off, Millipore) and purified by FPLC on a Superdex 200 column. Final protein was eluted in HBSC (HEPES Buffered Saline-Calcium buffer: 25m M HEPES-KOH, pH 7.4, 150 mM NaCl, 2 mM $CaCl_2$). PCSK9-containing fractions were pooled and concentrated approximately 5-fold. Purity of the protein was assessed by SDS-PAGE and Coomassie Brilliant Blue R-250 staining (Bio-Rad), concentration was estimated by BCA protein assay (Pierce).

2.2.4 LDL isolation

Human LDL was isolated from plasma as described previously[6]. Briefly, blood from healthy, fasted volunteers was collected in EDTA and plasma separated by low speed centrifugation. Protease inhibitors were added to the cleared plasma (1 mm PMSF and 50 units/liter aprotinin). VLDL (d = 1.006 g/ml), LDL (d = 1.019–1.065 g/ml), and HDL (d = 1.065–1.21 g/ml) were isolated from human plasma using sequential potassium bromide flotation ultracentrifugation[71] followed by extensive dialysis against phosphate-buffered saline (PBS) containing 0.25 mm EDTA. Protein concentrations in lipoprotein preparations were determined using a modified Lowry assay[72] .

2.2.5 Liposome production

1.04 μmoles DOPC (MW 786.15) and 0.26 μmoles DOPE (MW 744.04) dissolved in chloroform were mixed and dried under a stream of nitrogen gas (PC:PE molar ratio 80:20). The lipid cake was dehydrated in a vacuum desiccator for 1 hour, then the lipids resuspended in 4 ml Liposome buffer (25 mM HEPES, pH 7.4, 100 mM KCl, and 2.5 mM MgCl2) at 25°C with slow agitation for 1 hour. The lipids were subjected to five cycles of freeze-thawing using liquid nitrogen and a 25°C water bath, and then extruded through a 100 nm membrane using a Liposofast extruder (Avestin).

2.2.6 In vitro PCSK9-LDL binding assays using gradient ultracentrifugation

These assays were performed with conditioned media. Binding reactions (0.8 ml volume) each containing 400 µg LDL and 1 µg PCSK9 with 1% Ovalbumin in low-salt HBSC buffer (25 mM HEPES-KOH, pH 7.4, 75 mM NaCl, 2 mM $CaCl_2$) were incubated at 37°C for 1 hour. LDL-bound and free PCSK9 were then separated by Optiprep (iodixanol) gradient ultracentrifugation according to a modified version of a previously described protocol[73]. A 12% Optiprep sample solution was prepared by diluting 0.75 ml of each binding reaction with 0.29 ml of 60% Optiprep and 0.26 ml of 10 mm Tris, pH 7.4. The 12% sample was layered in a Thinwall Ultra-Clear 2.2 ml tube (Beckman Coulter) below a 9% Optiprep solution (0.7 ml) prepared in 10 mm Tris, pH 7.4. The tube was overlaid with 10 mm Tris, pH 7.4 (0.2 ml). The gradients were centrifuged in a TLS55 rotor (Beckman Coulter) at 39,000 rpm for 18 h at 4 °C. Light (600 µl), medium (750 µl), clear (200 µl) and heavy (800 µl) fractions were collected from each tube by aspiration from the upper layer. Equivalent amounts of middle and heavy fractions were resolved by SDS-PAGE on 8% acrylamide gels, and relative PCSK9 in each fraction was analyzed by western blotting.

2.2.7 PCSK9 Cellular uptake assays

HEK293 cells were cultured in Medium B to 70% confluency, then transiently transfected with wild-type human LDLR (pLDLR-17) using Lipofectamine 2000 according to manufacturer instructions. The next day, cells were treated with 10µg/ml PCSK9 from conditioned media in Medium F for 2 hour at 37°C. Cells were then washed in ice-cold PBS-CM (PBS with 1 mM MgCl2 and 0.1 mM CaCl2) and whole cell extracts were prepared in Tris Lysis Buffer (50 mm Tris-Cl, pH 7.4, 150 mm NaCl, 1% Nonidet P-40 (EMD Biosciences), 0.5% sodium deoxycholate, 5 mm EDTA, 5 mm EGTA, Complete™ protease

inhibitor mixture, 1 mm phenylmethylsulfonyl fluoride (PMSF)). Extract proteins were resolved on 8% SDS-PAGE and LDLR, PCSK9, transferrin receptor and actin were detected by western blotting.

For uptake assays done in the presence of LDL, HEK293 cells were cultured as above; however, they were transfected with ΔR6-LDLR using Lipofectamine 2000 as per manufacturer instructions. The next day, cells were treated with 1μg/ml Dylight800-labelled PCSK9, either wild-type or A44P mutant, with or without 500 μg/ml LDL. The Dylight800-PCSK9 and LDL treatments in Medium F were first pre-incubated at 37°C for 20-30 minutes before addition to cells. After treatment for 2 hours at 37°C, whole cell extracts were prepared and proteins analyzed by 8% SDS-PAGE and western blotting as described above. To check for PCSK9-LDL association, portions of the treatment pre-incubations were subjected to 0.7% agarose gel electrophoresis (electrode buffer: 90 mM Tris, pH 8.0, 80 mM Borate, 2 mM Calcium lactate) at 40 V for 2 hours. Labelled proteins were then visualized directly using a LI-COR Odyssey infrared imaging system (LI-COR Biosciences).

2.2.8 Cell-surface LDLR degradation assays

HepG2 cells were cultured to 60% confluency in Medium B, then cultured in sterol-depleting Medium D for 18-20 hours. Recombinant wild-type, A44P- or D374Y-PCSK9 was added to the medium and cells incubated at 37°C for 4 hours. Cells were then washed three times with ice-cold PBS-CM (PBS with 1 mM MgCl2 and 0.1 mM CaCl2) and once in Biotinylation buffer (10 mM triethanolamine, 2 mM CaCl2, 150 mM NaCl, pH 9.0). Cell-surface proteins were then biotinylated by incubating with 1 mg/ml EZ-link^{TM} Sulfo-NHS-S-S-biotin in Biotinylation buffer for 30 minutes at 4°C. Cells were washed once in Quenching buffer (192 mM glycine, 25 mM Tris in PBS-CM) and incubated for 10 minutes with quenching buffer

with light agitation. Cells were then rinsed twice with PBS-CM, scraped, and whole cell extracts prepared as described above. 50 µl Neutravidin agarose bead slurry and 1X Complete™ Protease Inhibitor was added to each cell extract, and rotated at 4°C for 16 hours. Neutravidin beads were pelleted at 400xg for 1min and washed three times in Tris Lysis Buffer (50 mM Tris-Cl, pH 7.4, 150 mM NaCl, 1% Nonidet P-40 (EMD Biosciences), 0.5% sodium deoxycholate, 5 mM EDTA, 5 mM EGTA) and once in 10 mM Tris, pH 7.4. Biotinylated proteins were eluted by boiling in sample buffer supplemented with 5% β-mercaptoethanol, and proteins were resolved on 8% SDS-PAGE and immunoblotted as above.

2.2.9 In vitro PCSK9-liposome binding assays

Recombinant wild-type or A44P-PCSK9-FLAG (300 ng) were incubated with 150 µl PC:PE (80:20) liposomes in Liposome buffer (25 mM HEPES, pH 7.4, 100 mM KCl, and 2.5 mM MgCl2) in final 200 µl volume. After incubation at 37°C for 1 hour, binding reactions were ultracentrifuged in Thickwall polycarbonate 230 µl tubes (7 x 21 mm, Beckman Coulter) in a TLA-100 rotor (Beckman Coulter) for 1 hour at 87,000 rpm. Supernatants were collected, and then liposome pellets were washed twice gently with Liposome buffer and resuspended in 100 µl Liposome buffer. 20 µl each of supernatant and pellet were resolved on 8% SDS-PAGE and PCSK9 detected by Western blotting.

2.2.10 Competition Binding Curves

These assays performed with purified protein. For each PCSK9 variant to be tested, a 12-reaction series was prepared where each reaction contained 0.5 mg/ml of LDL and 10.8 nM DyLight800-labelled wild-type PCSK9. To each reaction going down the series was added increasing amounts of unlabelled PCSK9 (either wild-type or R46L) upto a 500-fold excess

(highest 5000 nM). These reactions were incubated at 37℃ for 90 minutes in HBSC (HEPES Buffered Saline-Calcium buffer: 25 mM HEPES-KOH, pH 7.4, 150mM NaCl, 2mM CaCl2) and 1% BSA before being resolved on a 0.7% agarose gel (electrode buffer: 90 mM Tris, pH 8.0, 80 mM Borate, 2 mM Calcium lactate) at 40 V for 2 hours. Labelled proteins were then visualized using a LI-COR Odyssey infrared imaging system (LI-COR Biosciences). Intensity data was fit to a sigmoidal one-site binding curve using Graphpad Prism 5 software to obtain the inhibitor constant for each protein (K_i).

2.2.11 PCSK9-LDL Gel Shift Assays

120 ng of Dylight800 labelled wild-type or A44P-PCSK9 were incubated with 15 µg LDL in 30 µl volume reactions in low-salt HBSC buffer (25 mM HEPES-KOH, pH 7.4, 75 mM NaCl, 2m M $CaCl_2$) with 1% (w/v) bovine serum albumin. Binding was allowed to occur at 37°C for 1 hour, after which 10 µl of 4X Ficoll loading dye (10% (w/v) Ficoll400, 0.02% (w/v) bromophenol blue, 90 mM Tris, pH 8.0, 80 mM Borate, 2 mM Calcium lactate) was added to each reaction. 30 µl of each was resolved on a 0.7% agarose gel as described above. Labelled proteins were then visualized using a LI-COR Odyssey infrared imaging system (LI-COR Biosciences).

2.2.12 Statistical Analyses

All statistical analyses were carried out on Graphpad Prism 5 software. All experiments were repeated a minimum of 3 times, and all bar graphs report mean values with error bars showing standard error of the mean (SEM). Means were compared by paired, two-tailed student's t-tests or by one-way ANOVA followed by a post-test (Dunnett's test to compare all columns vs. control column, or Bonferroni's test to compare all column pairs).

3. Results

3.1 Alteration or deletion of key residues in the PCSK9 prodomain affect LDL binding but do not hinder LDLR binding.

3.1.1 N-terminal mapping of the PCSK9 prodomain

Specific features of interest in the N-terminal region were targeted for alteration by site directed mutagenesis (^{31}QEDEDGDYEELVLALRSEEDGL^{52}). A conserved stretch of acidic residues (^{32}EDEDGDYEE^{40}) was deleted while a conserved stretch of hydrophobic residues (^{41}LVLALR^{46}) was replaced with a disordered linker sequence (GGSGGS). A sulfation site (Y38) and a phosphorylation site (S47) were altered to either preserve or abolish the negative charge of the post-translational modification. Density flotation ultracentrifugation separated LDL-bound and non-LDL-bound PCSK9 from in vitro binding reactions between isolated human LDL particles and PCSK9 present in conditioned media of HEK293 cells transiently transfected with various PCSK9 plasmid constructs. The LDL-fraction and the heavy fraction (containing any free protein) from the centrifugation were analyzed for PCSK9 content by western blot (Figure 6B). An average of 30% of the wild-type PCSK9 was found in the LDL fraction under these in vitro assay conditions, closely approximating conditions in plasma where 30-40% of circulating PCSK9 was bound to LDL in normolipidemic humans[8].

Deletion of the entire N-terminal region of interest (Δ53) showed complete loss of LDL-binding, as expected. Deletion and disruption of both the acidic and hydrophobic stretch (Δ33-40 and GGSGGS-PCSK9 respectively) resulted in loss of LDL binding. Δ33-40-PCSK9 found in the LDL-fraction was reduced by 95%, while GGSGGS-PCSK9 was

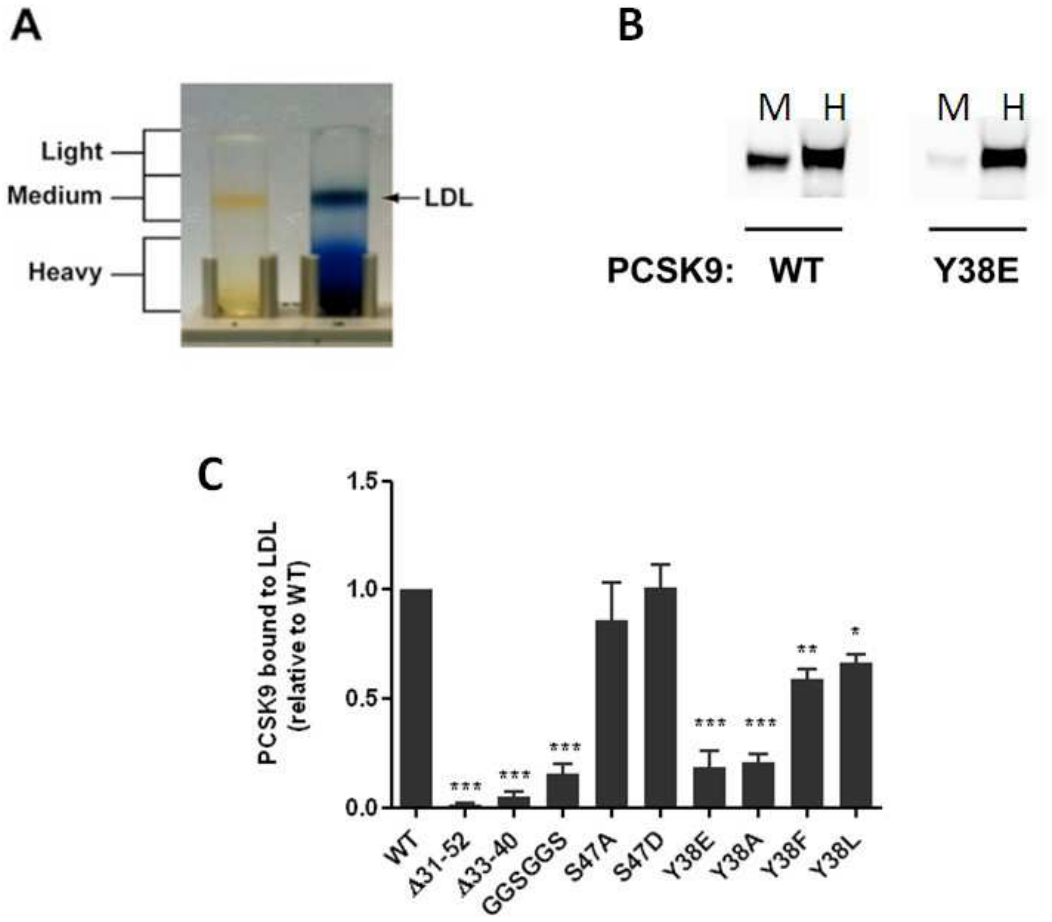

Figure 6: Mapping of the PCSK9 N-terminal region for LDL-binding. (A) Visual of a plasma sample subjected to density ultracentrifugation. Lipoproteins in the centrifuged sample separate according to their density, forming light (L), medium (M) and heavy (H) density fractions. LDL (seen in left tube), and any proteins bound to it (seen in Coomassie-stained right tube), are found in the medium fraction, while free protein and HDL is found in the heavy fraction. **(B) Example of western blot analysis of the medium (M) and heavy (H) fractions of ultra-centrifuged in vitro PCSK9-LDL samples.** 1 µg of PCSK9 and 400 µg LDL are allowed to bind *in vitro* for 1 hr at 37°C. LDL-bound and unbound PCSK9 are then separated using ultracentrifugation. Centrifugation fractions are then analyzed by western blot. A higher proportion of wild-type PCSK9 is seen in the LDL-containing (M) fraction than Y38E-PCSK9. **(C) Quantification of LDL-bound PCSK9**, showing proportion PCSK9 in M fraction relative to wild-type for n=3. Stars indicate a difference with the wild-type with *p<0.05, **p<0.01 and ***p<0.001 according to Dunnet's post-test after one-way ANOVA.

reduced by 85%. Neither abolishing the phosphorylation site with an alanine substitution (S47A), nor permanently preserving the negative charge of phosphorylation with an aspartate substitution (S47D) caused a notable change in the proportion of PCSK9 in the LDL fraction, suggesting that this residue does not hold an important role in LDL-binding. However, changing the tyrosine sulfation site to a negatively charged glutamate residue (Y38E) did cause a notable loss of LDL binding, reducing PCSK9 in the LDL fraction by 82%. Interestingly, a mutation to a phenylalanine (Y38F) – which is a residue identical to tyrosine except for the lack of a hydroxyl group where sulfation would normally occur - preserved LDL binding considerably, with a decrease of only 42% (Figure 6C). This led to the hypothesis that the hydrophobicity of the sulfation site, rather than the charge, was important for LDL binding. This hypothesis was tested by further mutating the Y38 to an alanine (less hydrophobic than phenylalanine) or a leucine (slightly more hydrophobic than phenylalanine). The Y38A mutant showed a lowered ability to bind LDL, decreasing by 79% from wild-type levels, while the Y38L mutant maintained LDL binding at levels comparable to Y38F, with a decrease of 34% compared to wild-type levels (Figure 6C). These findings further supported the importance of the hydrophobicity of the residue at position 38 in PCSK9-LDL binding.

3.1.2 Cellular LDLR-mediated uptake of targeted PCSK9 N-terminal variants

To confirm the proper folding and functionality of all the targeted prodomain mutants, their ability to bind cell surface LDLRs and undergo cellular uptake was evaluated in HEK293 cells over-expressing wild-type human LDLR. LDLR-transfected or non-transfected cells were treated with 10 μg/ml exogenous PCSK9-FLAG from conditioned media for 2 hours at 37°C, and the amount of PCSK9 internalized was evaluated by Western blotting of cell

lysates. All mutants showed LDLR-mediated internalization at levels comparable to wild-type PCSK9 (Figure 7). Although not statistically significant, the deletion of the entire N-terminal region (Δ53-PCSK9) or deletion of the acidic stretch (Δ33-40-PCSK9) show a visible trend towards increased affinity for the LDLR (Figure 7), with internalization levels at approximately 2.5 times and 1.8 times higher than wild-type respectively. This is in agreement with previous studies where Δ53-PCSK9 showed a 7-fold increase in affinity for the LDLR extracellular domain in vitro[25], while exogenous Δ33-40-PCSK9 treatment reduced LDL internalization in HepG2 cells, presumably through increased binding and degradation of LDLRs[60]. Conversely the replacement of the hydrophobic stretch appears to have a slight trend toward lower internalization, at about 50% less than wild-type levels (Figure 7). PCSK9 uptake was negligible in cells not transfected with LDLR construct, supporting the requirement of the PCSK9-LDLR interaction for uptake of PCSK9 in HEK293 cells. Since all the mutants showed a high degree of specificity in the interaction with LDLR and none showed a statistically significant difference from wild-type PCSK9 internalization levels, the folding and functionality of these mutants can be inferred to be normal.

3.2 Loss-of function variant R46L-PCSK9 binds LDL with similar affinity to wild-type PCSK9 in vitro.

In addition to the targeted mutations, the loss-of-function R46L polymorphism of PCSK9[67] was investigated for LDL binding. R46L is a polymorphism found commonly in heterozygotes of European Caucasian descent, with a frequency in the UK of nearly 3%[74]. European-American R46L carriers had a mean reduction in LDL-C of 21% in the Dallas Heart Study[75]. The change from arginine to leucine was of interest here because it effectively

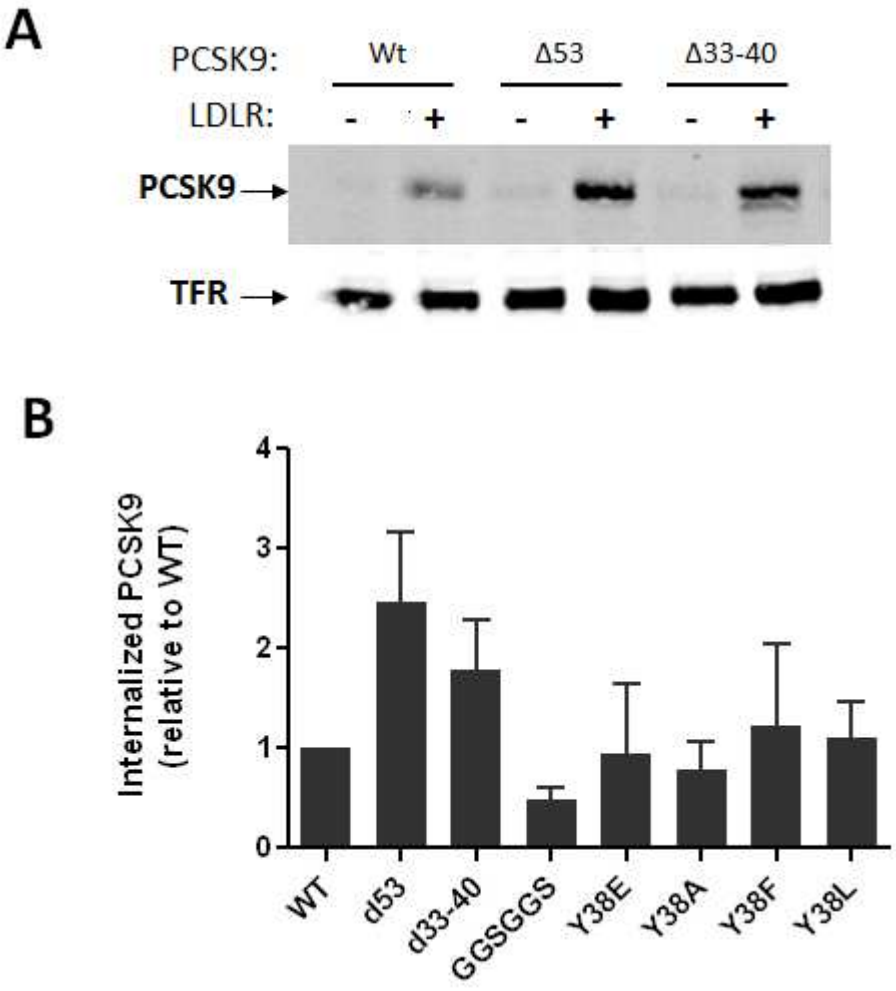

Figure 7: Cellular uptake of PCSK9 prodomain mutants in HEK293 cells. (A) Representative blot of internalized PCSK9. HEK293 cells transfected or not transfected with human wild-type LDLR were treated with 10μg/ml wild-type or mutant PCSK9-FLAG from conditioned medium for 2 hours at 37°C. Cells were then lysed and proteins resolved by SDS-PAGE and detected by western blotting. Shown are wild-type PCSK9 (WT), deletion of entire PCSK9 prodomain N-terminal (Δ53) and deletion of the acidic stretch (Δ33-40). Transferrin receptor was used as loading control. **(B) Quantification of internalized PCSK9-FLAG relative to wild type.** Plotted means for n=3 or n=4 with SEM.

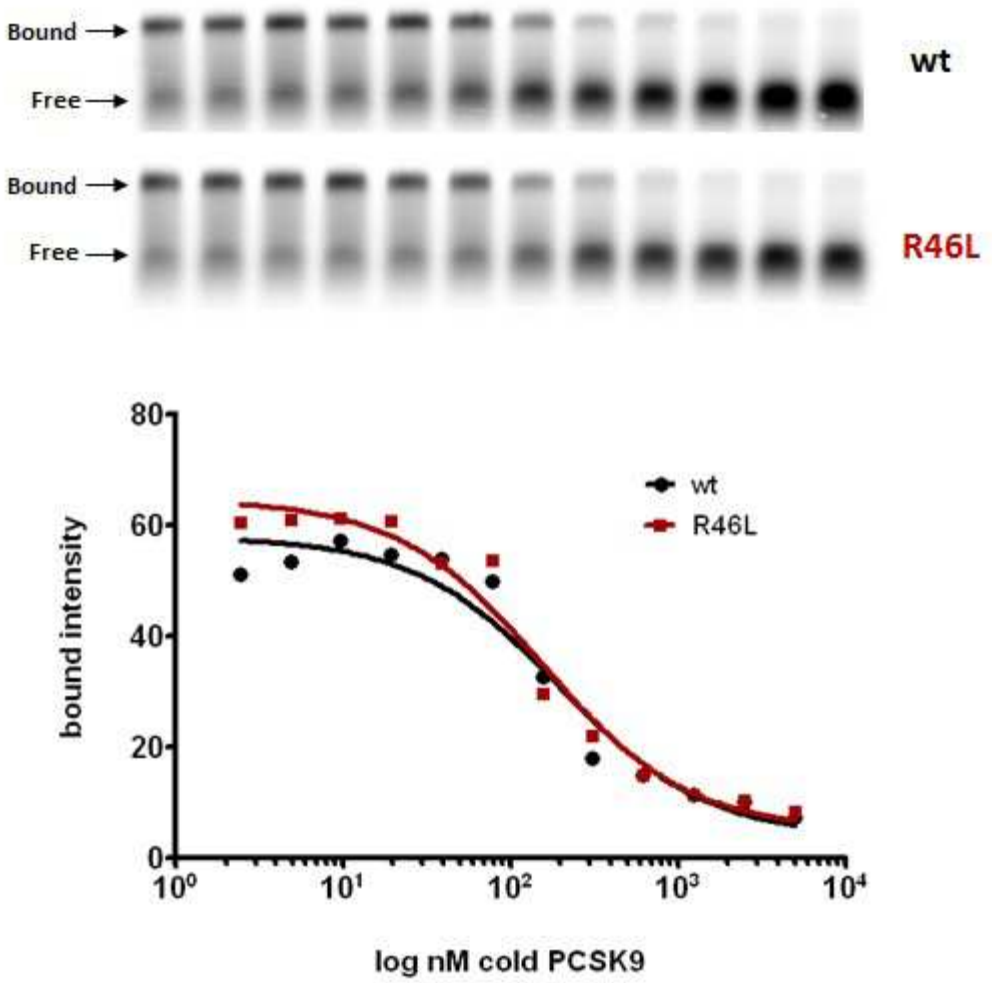

Figure 8: R46L PCSK9 competes for LDL binding with similar affinity to wt PCSK9 in agarose gel shift assay. 10.8nM IR-dye labelled PCSK9 was incubated with 500µg/ml LDL, in the presence of up to 500-fold excess unlabelled PCSK9, either wild-type or R46L. Bound and free complexes were resolved by electrophoresis on 0.7% agarose gels. Gels were visualized on a LI-COR Odyssey system. Bound labeled PCSK9 was quantified and fit to a one-site binding curve on Prism5 software using non-linear regression. A K_i of 197.9±85 nM was obtained for wild-type while a K_i of 162.4±51.6 nM was obtained for R46L. A representative agarose gel of three experiments is shown, while average data of n=3 is plotted on the binding curve.

extends the hydrophobic stretch in the prodomain, possibly affecting LDL association. Competition binding analysis was used to quantitatively assess the affinity of purified R46L for LDL compared to wild type. Dylight800-labelled wild-type PCSK9 was incubated with LDL in the presence of increasing concentrations, up to a 500-fold excess, of unlabelled competitor protein (either wild-type or R46L-PCSK9). Both wild-type and R46L-PCSK9 successfully competed dye-labelled PCSK9 for LDL binding sites, with bound 800-PCSK9 decreasing by approximately 90% at the highest concentration of unlabelled competitor (Figure 8). LDL-bound PCSK9 intensity data was fit to one-site sigmoidal binding curves with $R^2 > 0.95$. Inhibitor constants (K_i) were obtained from these binding curves. The K_i for wild-type PCSK9 competition was 197.9±85 nM, while the K_i for R46L competition was 162.4±51.6 nM. A student's t test revealed no significant difference between the wild-type and R46L K_is.

3.3 Mouse-PCSK9 retains the ability to bind human LDL

Within the amino acid 31-52 region of interest, the prodomain sequence of mouse PCSK9 bears 80% similarity to the prodomain sequence of human PCSK9, with the acidic and hydrophobic stretches fairly well conserved aside from a few conservative residue changes (Figure 9A). The replacement of a proline in the mouse instead of the positively charged R46 residue in the human is the only drastic change in terms of both side chain structure and polarity. A methionine (mouse) instead of the valine (human) at position 42 within the hydrophobic stretch represents a slight change in side-chain structure, with no difference in polarity of the residue. At human position 48, a glutamine in the mouse sequence instead of the glutamate in the human represents a decrease in acidity compared to human, but remains

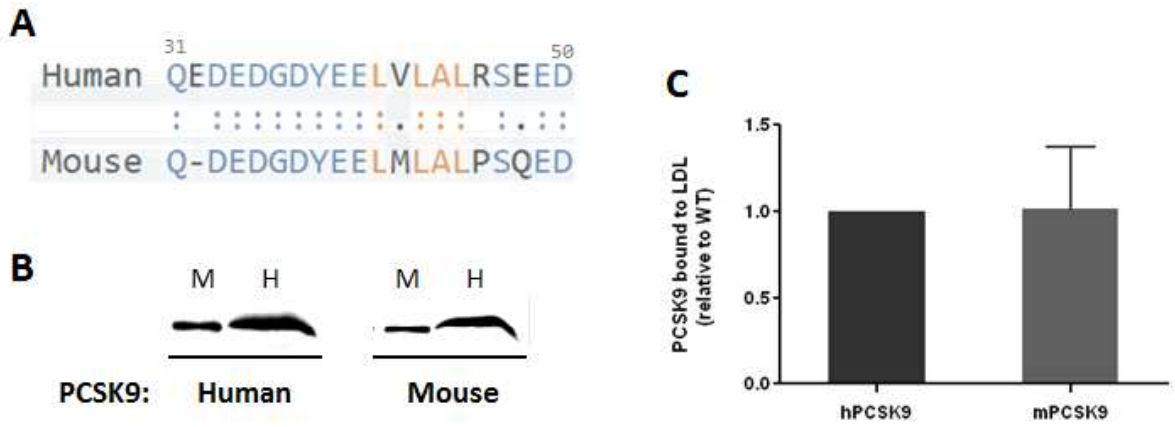

Figure 9: Mouse PCSK9 binds human LDL. (A) Amino acid sequence alignment of the N-terminal region of mouse and human PCSK9. Blue denotes conserved acidic stretches of residues while orange denotes the conserved hydrophobic stretch. **(B) Western blot of density-ultracentrifugation fractions of in vitro PCSK9-LDL binding reactions.** Proportion of PCSK9 present in the LDL-containing M fraction is comparable between mouse and human. Heavy (H) fraction contains free PCSK9. (C) Proportion PCSK9 in M fraction as quantified for n=3, relative to human. Graph showing means with SEM.

a structurally conservative change. A single glutamate residue missing in the mouse acidic stretch also contributes to making the mouse N-terminal slightly less acidic than the human. To investigate whether these more subtle differences in N-terminal sequence and acidity would affect LDL binding, in vitro evaluations of wild-type human and mouse PCSK9 LDL-binding were carried out using the density ultracentrifugation method as described above. It was found that mouse PCSK9 retained the ability to bind human LDL, with no difference in the proportion of LDL-bound PCSK9 between the two (Figure 9B, C). Thus the differences in prodomain N-terminal sequence between mouse and human PCSK9 do not affect LDL binding.

3.4 Helix-disrupting residues in the PCSK9 prodomain N-terminal region abolish LDL-binding but do not affect LDLR binding or degradation.

3.4.1 Introduction of proline residues into the prodomain N-terminal region abolishes LDL binding.

The importance of the hydrophobicity of the Y38 position, located in an otherwise negatively charged stretch, as well the positioning of this residue 3 amino acids away from the conserved hydrophobic stretch (as seen in N-terminal mapping section above), raised the possibility that the N-terminal region, which normally appears structurally disordered in crystal structures[25, 46-48], may form a lipid-ordered amphipathic helix in proximity to LDL, with the Y38 ending up on the hydrophobic face. Helical wheel modeling of segments of the N-terminal region showed that a helix that is amphipathic in nature could conceivably form, with the Y38 indeed in the middle of the hydrophobic face of the helix (Figure 10A).

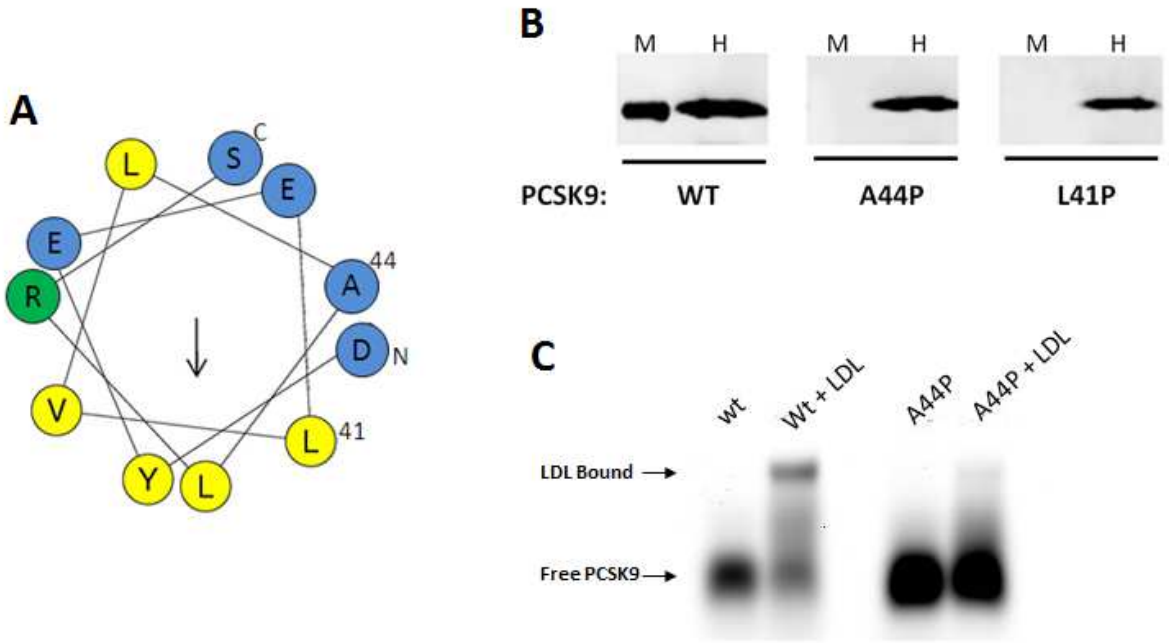

Figure 10: Introduction of helix-disrupting proline residues into PCSK9 prodomain N-terminal cause loss of LDL-binding. (A) Helical wheel model of mid-section of the N-terminal region (^{37}DYEELVLALRS^{47}). The N and C terminal are indicated, as well as the A44 and L41 residues that were mutated to prolines. Arrow indicates direction of hydrophobic moment. Yellow residues indicate hydrophobic residues, blue denotes polar or negatively charged residues, green indicates a positively charged residue. Model constructed on Heliquest. **(B) Western blot of density-ultracentrifugation fractions of in vitro PCSK9-LDL binding reactions.** 1 µg of PCSK9 and 400 µg LDL were allowed to bind in vitro for 1 hr at 37°C. LDL-bound and unbound PCSK9 were then separated using ultracentrifugation as described in Figure 1. Wild-type PCSK9 is seen present in the LDL-containing (M) fraction, but not the A44P or L41P-PCSK9 mutants. Similar results obtained for n=3. **(C) Agarose gel shift assay of Dylight800-labelled wild-type or A44P-PCSK9 with or without LDL.** 4 µg/ml labelled PCSK9 was incubated with 500 µg/ml LDL at 37°C for 1 hour. LDL-bound and unbound PCSK9 was resolved on 0.7% agarose. Fluorescently labelled proteins were directly visualized in the agarose on a LI-COR system. Similar results obtained for n=3.

To test the possibility of the existence of the helix, two helix-disrupting proline mutations were introduced into the N-terminal region near the interface of the putative hydrophobic and hydrophilic faces: A44P and L41P. LDL-binding of the PCSK9 mutants in conditioned medium was again assessed in vitro using density ultracentrifugation. It was observed that the proline mutations completely abolished binding to LDL, with no immunodetectable PCSK9 in the LDL fraction (Figure 10B). This supports the possibility of an amphipathic helix in this region aiding LDL association.

The loss of LDL-binding of A44P-PCSK9 was also demonstrated by an agarose gel shift assay where 4 μg/ml Dylight800-labelled PCSK9 (wild-type or A44P) was incubated with 500 μg/ml LDL at 37°C for an hour, then LDL-bound and free PCSK9 was resolved by agarose gel electrophoresis. A strong shift upward to a higher molecular weight was observed for wild-type LDL in comparison to the negative control lacking LDL. In contrast, nearly all A44P-PCSK9 incubated with LDL failed to shift upwards, with a migration identical to the no-LDL control. It should be noted, however, that using this technique, very low levels of upward-shifted A44P can be detected when incubated with LDL, at the same migration level as the wild-type PCSK9-LDL complex (Figure 10C). Quantification of the upward-shifted bands reveals an LDL-bound A44P signal that is an average of 83.6% less than that of the wild-type signal.

3.4.2 A44P- and L41P- PCSK9 undergo LDLR mediated cellular uptake similar to wild-type PCSK9.

Similar to the prodomain mapping mutants, the folding and functionality of the proline mutants was verified by their ability to be taken up by cells in an LDLR-dependent manner.

HEK293 cells transiently transfected with human wild-type LDLR were treated with 10 μg/ml exogenous wild-type or mutant PCSK9-FLAG from conditioned media for 2 hours at 37°C. Cell lysate proteins were then analyzed by SDS-PAGE and western blotting. Both mutants as well as the wild-type PCSK9 showed specific LDLR-mediated uptake. Levels of internalized A44P or L41P PCSK9 were comparable to wild-type levels, with no significant differences (Figure 11A).

3.4.3 A44P-PCSK9 mediates cell-surface LDLR degradation similar to wild-type PCSK9.

To further test the functionality of A44P-PCSK9, we investigated whether it retained the ability to mediate degradation of cell-surface LDLRs. HepG2 cells were induced to upregulate their cell-surface LDLR expression with pravastatin treatment for 18 hours. The cells were then treated with 10 μg/ml exogenous purified wild-type or A44P-PCSK9, or 2 μg/ml gain-of-function D374Y-PCSK9 for 4 hours at 37°C. Cell-surface proteins were biotinylated and isolated by pull-down with Neutravidin agarose beads, then detected by western blot.

As expected, the level of cell-surface LDLRs was observed to decrease in response to exogenous purified PCSK9 treatment. Treatment with 10μg/ml of wild-type PCSK9 reduced PCSK9 by 71%, while 10 μg/ml A44P-PCSK9 treatment reduced LDLR by 73% (Figure 11B). LDLR levels for all PCSK9-treated cells were statistically different from untreated cells. However, no statistically significant difference was found between the levels of LDLR degradation for the wild-type and A44P-PCSK9 treatments. This indicates that the A44P mutation does not affect the functionality of PCSK9. Gain-of-function D374Y-PCSK9 has a

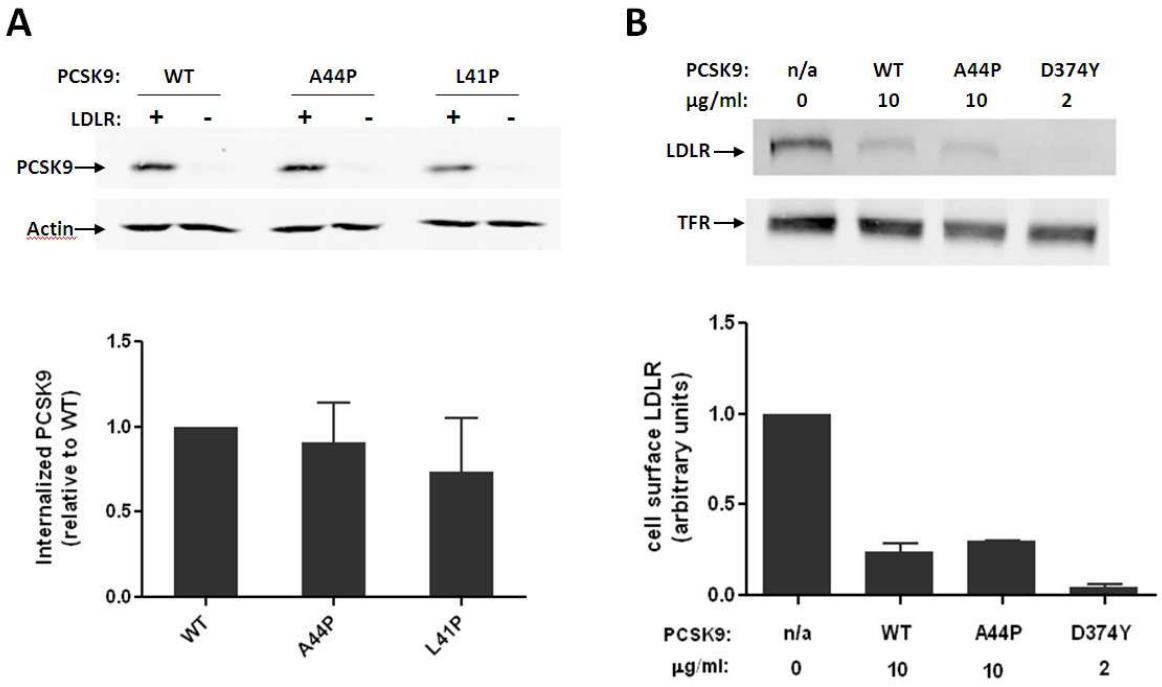

Figure 11: PCSK9 with proline mutations in the prodomain N-terminal region undergo LDLR-dependent cellular uptake and mediate LDLR degradation similar to wild-type PCSK9. (A) LDLR-dependent cellular uptake of exogenous PCSK9-FLAG in HEK293 cells. HEK293 cells transfected or not transfected with human wild-type LDLR were treated with 10 µg/ml wild-type or mutant PCSK9-FLAG from conditioned medium for 2 hours at 37°C. Cells were then lysed and proteins resolved by SDS-PAGE and detected by western blotting. Actin was used as loading control. Graph showing means of n=3 with SEM, relative to wild-type. **(B) Cell-surface LDLR degradation by exogenous PCSK9-FLAG.** HEPG2 cells induced to upregulate LDLR expression by pravastatin treatment were treated with purified exogenous wild-type, A44P- or D374Y- PCSK9-FLAG for 4 hours at 37°C. Cells-surface proteins were then biotinylated and isolated by pulldown with Neutravidin agarose beads, resolved by SDS-PAGE and detected by western blot. Plotted means of n=3 with SEM, relative to no treatment (n/a). All lanes are significantly different from no treatment ($p<0.001$) according to Bonferroni's post-test after one-way ANOVA.

10-fold higher LDLR-affinity than wild-type PCSK9[55], and serves here as a positive degradation control. As expected, D374Y treatment was the most efficient at causing LDLR degradation, with a 2 μg/ml treatment decreasing LDLRs by 97% (Figure 11B).

3.5 PCSK9 shows lipid association, disrupted by the A44P mutation

If a lipid-ordered amphipathic helix were to develop in the N-terminal of the PCSK9 prodomain in proximity to LDL, it is possible that the helix could play a role in PCSK9 docking onto the lipid portion of LDL to aid the eventual binding of PCSK9 to its preferred site on ApoB. Thus, we aimed to investigate whether wild-type PCSK9 could associate with lipids in the form of liposomes. We also aimed to investigate whether the A44P mutation would affect this lipid association.

Co-pelleting assays were used to assess the extent of PCSK9 association with liposomes. A mixture of phosphatidylcholine and phosphatidylethanolamine in an 80:20 molar ratio was extruded through a 100 nm pore-sized membrane to form liposomes. Conditioned medium containing either wild-type or A44P-mutant PCSK9 was incubated with the liposomes at 37°C for an hour before being subjected to ultracentrifugation, which pellets liposomes, but leaves any free, non-lipid bound protein in the supernatant (Figure 12A). PCSK9 content in the pellet and the supernatant could then be evaluated by western blot.

It was observed that wild-type PCSK9 was consistently found in the pellet fraction, indicating that PCSK9 is capable of associating with liposomes. The A44P mutant consistently showed an absence or greatly decreased presence in the pellet fraction, suggesting that the presence of a helix-disrupting proline residue in the N-terminal region

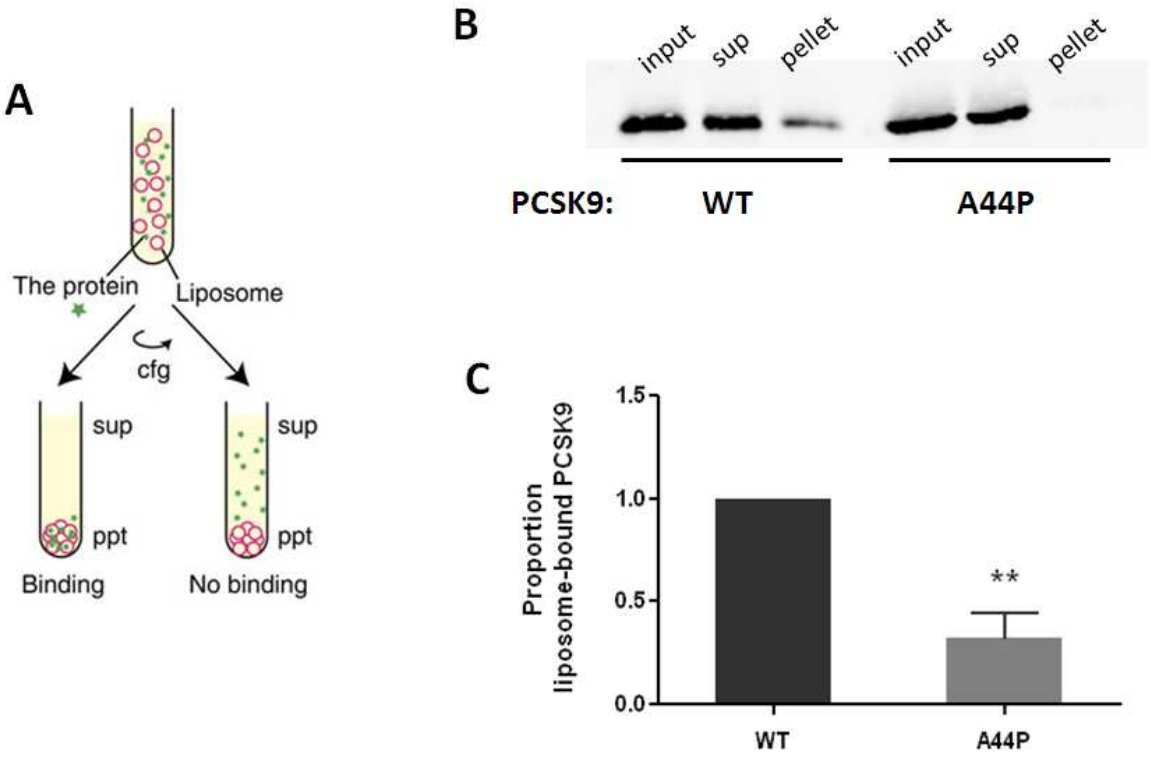

Figure 12: Investigation of PCSK9-liposome association and effects of the A44P mutation. (A) Schematic of PCSK9-liposome co-pelleting assay. After incubation, in vitro PCSK9-liposome binding reactions are ultracentrifuged so that the liposomes, with any bound proteins, are pelleted; soluble free protein remains in the supernatant. Panel adapted from Nobuaki *et al*, 2014[85]. **(B) Representative western blot of co-pelleting fractions.** Showing inputs (before centrifugation), supernatants and pellets from co-pelleting assays using wild-type or A44P-PCSK9 mutant conditioned media. **(C) Quantification of co-pelleting fraction western blots.** The pellet:supernatant ratio of protein was calculated from western blot quantifications and plotted means with SEM relative to wild-type (n=5). Two stars indicate a difference from the wild-type with $p<0.01$ according to student's t test.

may be negatively affecting lipid association (Figure 12B). Averaging quantifications from n=5, A44P-PCSK9 association with lipids is found to be decreased by 80% compared to wild-type binding. This result further suggests that a lipid-ordered helix may play a role in PCSK9 docking onto the phospholipid exterior of LDL before finding its protein-protein binding site on ApoB.

3.6 Cellular uptake of A44P-PCSK9 and Δ53-PCSK9 in presence of LDL.

The presence of LDL is inhibitory to PCSK9-LDLR binding and to the LDLR-degrading activity of PCSK9. With 500 μg/ml LDL, LDLR levels recover by 90%, while the cellular uptake of PCSK9 is inhibited by >70% in HuH7 cells treated with exogenous gain of function D374Y-PCSK9-FLAG[6]. If the A44P mutation disrupts a putative helical structure important for LDL-binding, and Δ53-PCSK9 (deletion of entire N-terminal region) lacks this structure completely, it would be expected that the activity of these mutants would no longer be regulated by LDL.

In order to test this hypothesis, the cellular uptake of Dylight800-labelled PCSK9-FLAG was investigated in the presence or absence of LDL. HEK293 cells were transiently transfected with a mutant form of the LDLR, namely, ΔR6-LDLR. ΔR6-LDLR contains a deletion of structural repeat number 6 in the ligand binding domain of the LDLR, mimicking a natural mutation in the LDLR that is defective in LDL-binding[76].This eliminated the possibility that any effects observed on the PCSK9-LDLR interaction are due to LDL binding to the LDLRs. PCSK9 binding to ΔR6-LDLR is comparable to wild-type LDLR[6]. 1 μg/ml wild-type, A44P-

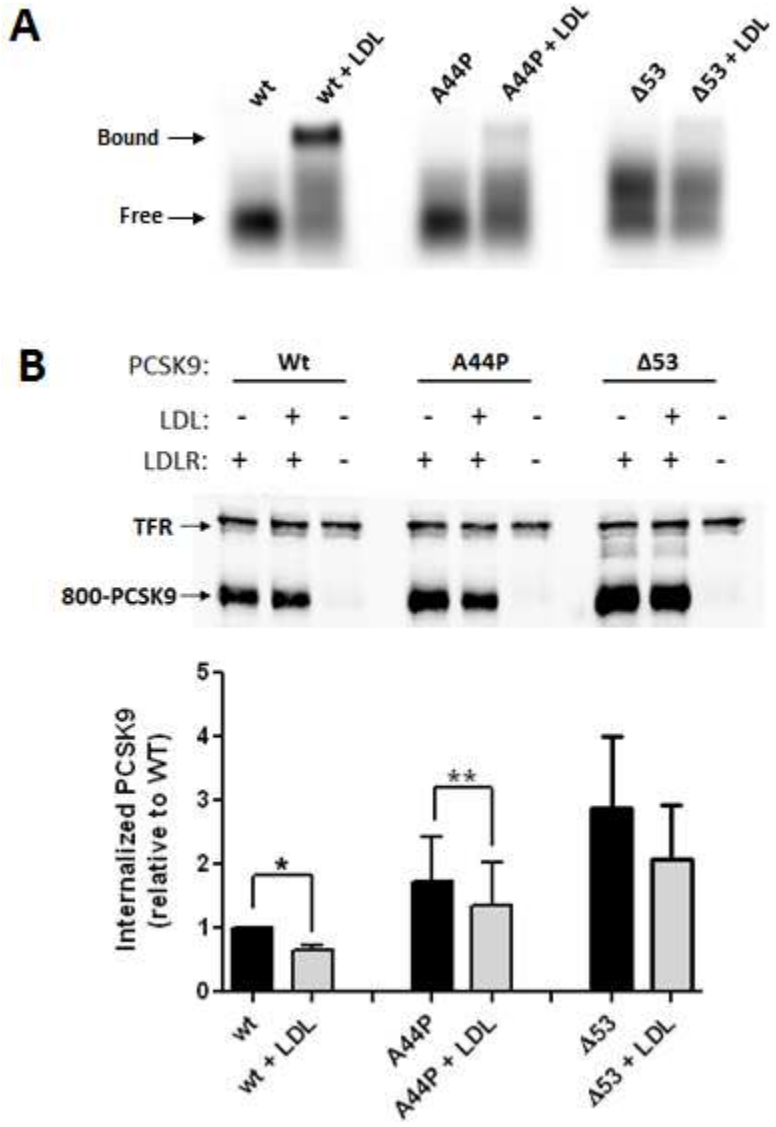

Figure 13: Wild-type, A44P- and Δ53-PCSK9 cellular uptake in the presence of LDL. HEK293 cells were transfected with ΔR6-LDLR (LDLR with deletion of ligand-binding repeat #6) to remove any effect of the LDL-LDLR interaction. Cells were then treated with 1 µg/ml Dylight800-labelled wild-type, A44P- or Δ53-PCSK9 for 2 hours at 37°C. **(A)** Before addition to cells, PCSK9+LDL treatments in medium were pre-incubated at 37°C for 30 minutes and portions resolved on 0.7% agarose to confirm PCSK9-LDL association. **(B)** Cell lysates were analyzed for internalized PCSK9 by SDS-PAGE and detection on a Licor system. Quantification shown immediately below. Star indicates $p<0.05$, two stars indicate $p<0.01$with student's t test.

or Δ53- Dylight800-PCSK9-FLAG was pre-incubated with or without 500 µg/ml LDL at 37°C for 30 minutes in order to ensure PCSK9-LDL binding would reach equilibrium. ΔR6-LDLR -transfected cells were then treated with the pre- incubated PCSK9-LDL mixtures for 2 hours at 37°C. Cell lysates were analyzed for internalized PCSK9 by western blotting.

In order to ensure that the PCSK9 was able to associate with LDL in the pre-incubation conditions, portions of the pre-incubations were subjected to agarose-gel electrophoresis and Dylight labelled PCSK9 visualized directly in the agarose using an infrared LI-COR scanner. The results reveal that the wild-type PCSK9 does associate with LDL as expected, showing a strong upwards shift in the LDL-lane. A44P-PCSK9, again as expected, shows a decrease from wild-type of 90 % in the LDL-shifted band (Figure 13A). These results indicate that the ability of the Dylight800-labelled PCSK9 to associate normally with LDL during cell treatment is not impaired, and the A44P mutation maintains its relative inability to bind LDL. Δ53-PCSK9, as has been observed in the lab in the past, does not migrate normally in agarose, appearing to form an aggregate band which migrates higher than the free-PCSK9 band seen for wild-type and A44P-PCSK9, but lower than the LDL-shifted band seen for wild-type or A44P-PCSK9. No LDL-shift occurs for Δ53-PCSK9.

With respect to cellular uptake, wild-type PCSK9 showed a decrease in LDLR-dependent cellular internalization in the presence of LDL, as expected (Figure 13B). However, this represented a 36% decrease, in contrast to previous studies where wild-type PCSK9 uptake was decreased by >70% in the presence of 500 µg/ml LDL. There are notable differences in cell culture between this experiment and the study by Kosenko *et al*, where they used HuH7 cells instead of HEK293, and uptake incubation time was 4 hours instead of 2 hours, with the

use of chloroquine to prevent lysosomal protein degradation. These experimental differences may account for some of the differences in wild-type PCSK9 response to LDL.

For Δ53-PCSK9, a trend towards a 24% decrease in uptake in the presence of LDL was observed. Although from our in vitro results showing complete loss of LDL-binding, a more robust loss of inhibition by LDL would be expected for Δ53-PCSK9 (Figure 6C), this decrease is slightly less than the 36% decrease obtained with wild-type PCSK9. The differences in Δ53-PCSK9 uptake between LDL and no-LDL treatments were also not statistically significant. Similarly, A44P-PCSK9 showed an inhibition of cellular uptake of 30% in the presence of LDL. This decrease was statistically significant, although still a smaller decrease than that of wild-type. Thus, while A44P- and Δ53-PCSK9 do not show robust losses in regulation by LDL, they show slight trends towards higher levels of LDLR-binding in the presence of LDL compared to wild-type PCSK9.

4. Discussion

PCSK9 is an important negative regulator of cell-surface LDLR levels, thus regulating circulating LDL-cholesterol levels. The purpose of this project was to examine the recently discovered interaction between PCSK9 and LDL. Indirect evidence of PCSK9 association with lipoproteins began coming out in 2008, when Fan *et al*, and later Luo *et al* carried out size exclusion chromatography studies where PCSK9 co-migrated with LDL-sized particles[77, 78]. However, there are large macromolecular complexes present in plasma (e.g. α2-macroglobulin) that could contain PCSK9 and co-migrate with LDL at the limited resolution of size-exclusion chromatography. Positive identification of PCSK9 binding to LDL in human plasma came from more detailed studies, which utilized density gradient

separations to isolate an LDL fraction that was shown to contain PCSK9[6,8]. Importantly, >30% of circulating PCSK9 was found to be associated with LDL in normolipidemic human plasma, suggesting a significant role of LDL-association in regulating PCSK9 function.

Direct binding assays and mammalian two-hybrid assays support that PCSK9-LDL association likely occurs through a protein-protein interaction between PCSK9 and ApoB[6, 7], although a specific binding site on either protein has not yet been established. In vitro work has also shown that the PCSK9-LDL interaction is capable of inhibiting the ability of PCSK9 to bind and degrade LDLRs in cultured hepatic cells, and that this inhibition does not occur through competition of LDL and LDLR for a common binding site[6]. What mechanism causes this inhibition has yet to be elucidated. We hypothesized that an N-terminal region of the PCSK9 prodomain is involved in an allosteric mechanism regulating PCSK9 activity. This hypothesis was based on the finding that deletion of the prodomain N-terminal residues 31-52 caused a loss of PCSK9-LDL binding[6]. As well, previous studies had found the same N-terminal region to be autoinhibitory to the PCSK9-LDLR interaction and the LDLR-degrading activity of PCSK9[25, 60]. We further hypothesized that LDL-binding may stabilize an inhibited form of PCSK9, which, in equilibrium with non-lipoprotein bound PCSK9, would regulate the level of PCSK9 activity in circulation and contribute to plasma cholesterol homeostasis.

4.1 Specific residues within the prodomain N-terminal are crucial for PCSK9-LDL binding.

While the N-terminal region from residue 31-52 in the PCSK9 prodomain have been shown to be required for LDL binding[6], it was not known whether specific residues within this region had a role in the interaction. Here we report that the 9-residue stretch of acidic

residues and the adjacent 5-residue hydrophobic stretch in the PCSK9 prodomain N-terminal, were both important for the PCSK9-LDL interaction (Figure 6C). Both of these regions are well conserved among species; across primates, rodents and zebrafish[60]. This involvement of both charged and hydrophobic residues in close proximity led us to perform helical wheel modelling of the region, and the discovery that a helix exhibiting an amphipathic pattern could form in the region (Figure 10A). The hydrophobic face of an amphipathic helix may confer lipid-binding capabilities, such as to the phospholipid exterior of lipoproteins. Interestingly, we also found that at position 38 (Y38), the hydrophobicity of the residue was the important feature aiding LDL-binding. As seen in Figure 6C, substitution of the tyrosine-38 with hydrophobic residues (phenylalanine and leucine) preserved LDL-binding to a greater extent than the less hydrophobic (glutamate and alanine) substitutions. This was particularly interesting because the tyrosine-38 is a sulfation site[51], carrying a negative charge once sulfated. Given that position 38 is located within the acidic stretch it would at first seem intuitive that the acidity of residue 38 would have a role in LDL-binding, possibly regulating the protein-protein interaction with ApoB. However, the helical wheel model places the Y38 residue in the middle of the hydrophobic face of the helix, which would explain why it is the hydrophobicity of the site that matters. What proportion of PCSK9 secreted from the liver is normally sulfated has not yet been studied, thus it is not clear whether Y38 sulfation may have a role in regulating PCSK9-LDL association in vivo. Our results also suggest that presence or absence of the phosphorylation site at S47 does not affect LDL binding (Figure 6C). PCSK9 is found as a phosphoprotein in human plasma although the phosphorylation of PCSK9 in plasma is not 100%[52].

The mutations studied for the mapping maintain their ability to bind LDLRs and undergo LDLR-mediated cellular uptake (Figure 7), suggesting that these mutations do not disrupt the global structure of PCSK9. Rather, they specifically implicate these residues in the regulation of the LDL interaction. The loss of LDL-binding caused by the above mentioned mutations thus become interesting in the context of the proposed allosteric mechanism regulating the PCSK9-LDL interaction and the subsequent regulation of PCSK9 activity.

The requirement of the N-terminal region for PCSK9-LDL binding does not confirm whether the physical binding site of ApoB lies in this region or whether this region is simply a conformational or allosteric modulator of the interaction, with the protein-protein interaction site lying elsewhere in the PCSK9 protein. If the binding site were to lie outside of the prodomain N-terminal it would most likely be in the solvent exposed C-terminal domain, containing a section rich in cystein & histidine residues and carrying a net positive charge. It is unlikely that LDL binds in the PCSK9 catalytic domain since it was found that large LDL particles do not sterically interfere with the PCSK9-LDLR EGF-A interaction in vitro[6]. The EGF-A binding site on PCSK9 takes up a considerable surface area on the catalytic domain[25], leaving the prodomain and the C-terminal domain as the most likely regions of the protein that would allow unhindered simultaneous LDL and LDLR binding. There is also the possibility that residues in the positively charged C-terminal domain form an intramolecular interaction with the negatively charged acidic stretch in the N-terminal domain. This might interfere with secondary interactions of the C-terminal domain with the LDLR, thus playing a role in the autoinhibitory function of the N-terminal region of the prodomain.

The N-terminal region of the PCSK9 prodomain is normally exposed to solvent but structurally disordered[46-48]. The formation of a lipid-ordered amphipathic helix in close

proximity to LDL could conceivably aid the docking of PCSK9 onto the phospholipid exterior of lipoproteins, allowing it to more easily come into contact with its binding site on ApoB. Proteins such as the phospholipid biosynthetic enzyme CCTα are known to have lipid or membrane-binding domains that switch from random coils to α-helical structure in contact with lipids[79]. Conservative changes in the overall sequence or polarity of the N-terminal region do not affect LDL-binding, as demonstrated by the ability of mouse PCSK9 to associate with LDL to the same extent as human PCSK9 (Figure 8). Notably, the conservative changes between mouse and human PCSK9 would not greatly affect the amphipathic nature of the putative N-terminal helix, which perhaps may help to conserve the binding of mouse PCSK9 to human LDL. It is also interesting to note that mouse PCSK9 contains a proline near the end of the sequence appearing in the helical wheel model (Figure 9A, 10A). While proline residues within helices can be disruptive to helical structures, prolines also make good C-terminal caps that stabilize helices at their ends[80].

4.2 A model for PCSK9 docking onto lipoproteins through an amphipathic helix

We found further support for the N-terminal helix concept from the substitution of proline residues for the A44 and L41 residues in the N-terminal region. Both of these positions lie near the interface of the hydrophobic and hydrophilic faces of the putative helix (Figure 10). Proline residues are normally disruptive to alpha helical structures, and insertion of proline into the N-terminal region would presumably disrupt any helix that may form in proximity to lipids. We found that both the A44P and L41P mutations, which did not otherwise disrupt PCSK9 functionality (Figure 11), greatly decreased the ability of PCSK9 to bind to LDL (Figure 10 B,C). This supported that a helical structure in the region was indeed disrupted, and that the disrupted structure holds an important role specifically in LDL binding.

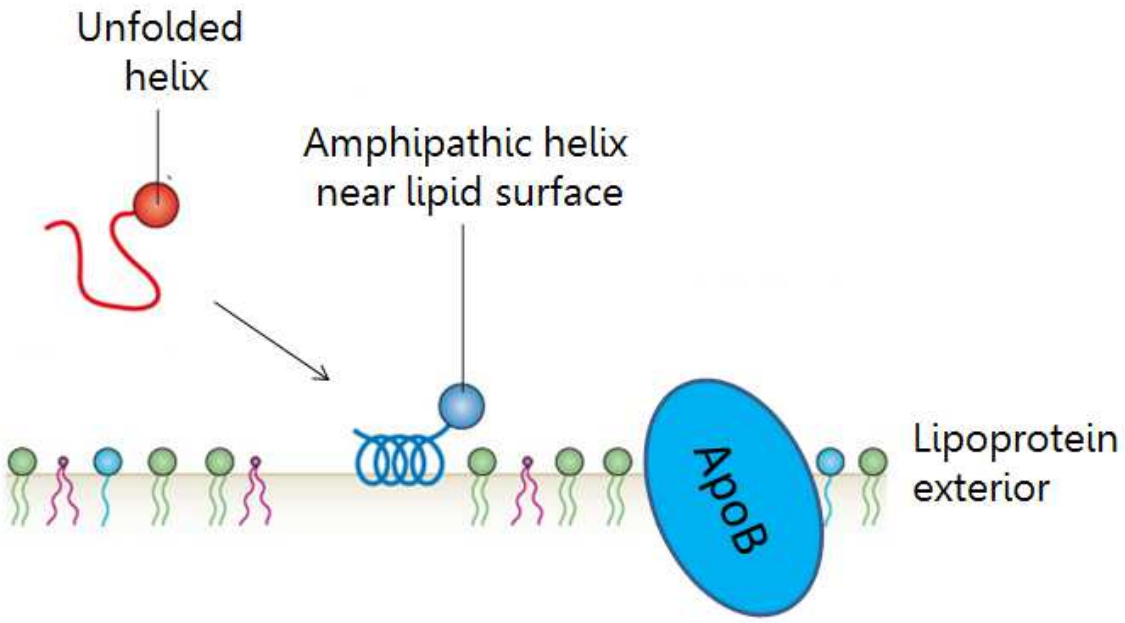

Figure 14: Model for PCSK9 docking onto lipoprotein surfaces with the help of a lipid ordered amphipathic helix. While free in circulation, the solvent exposed prodomain N-terminal of PCSK9 remains disordered. In proximity to lipoprotein surfaces, the N-terminal adopts a lipid-ordered helical structure that allows PCSK9 docking onto the phospholipid surface and search for its binding site on ApoB100. Figure adapted from Thiam *et al*, 2003[81].

PCSK9 binds to LDL but not to VLDL[6], even though VLDL contains ApoB100. It is possible that as VLDL is catabolised and remodelled in the circulation by lipoprotein lipase to IDL and LDL, different epitopes and binding sites on ApoB are exposed and become available for PCSK9 binding. ApoB on LDL may have the preferred binding site for PCSK9 available whereas ApoB on VLDL may not. An amphipathic helix on PCSK9 conferring lipid-association would likely aid docking of PCSK9 onto the lipid portion of a variety of different lipoproteins, allowing PCSK9 to scan the lipoprotein surface for its binding site on ApoB. We found evidence for the ability of PCSK9 to associate with lipids, where wild-type PCSK9 was found to associate with liposomes composed of phospholipids commonly found in LDL particles (phosphatidylcholine and phosphatidylethanolamine) (Figure 12). As would be expected from our previous LDL-binding results, a proline-containing PCSK9 mutant was found to have decreased ability to bind liposomes (Figure 12), again supporting the notion that a helical structure is important for the association of PCSK9 with lipids.

The lipid association of PCSK9 also opens up another interesting possibility of PCSK9 targeting to LDL particles, i.e. the composition and packing of the lipid surface of the lipoprotein. Apolipoproteins such as ApoA-I or ApoC-I are known to associate with lipid surfaces using amphipathic helices, and are dependent upon surface packing and composition for targeting to these surfaces[81]. CCTα is known to form α-helices in its membrane binding domains only in the presence of anionic lipids[79]. Future liposome-binding experiments using a variety of liposome compositions may shed further light on these lipid-targeting mechanisms in the case of PCSK9.

Evidence from previous studies indicating that PCSK9 binds to LDL through a specific, one-site protein-protein interaction with ApoB[6, 7] does not show a role for lipid- binding in

the PCSK9-LDL interaction. However, it should be noted that the suggested helix (Figure 10) is composed of a relatively short stretch of residues and would form a small helical region. It is likely that its lipid-binding and docking function is relatively weak and transient, where PCSK9 easily dissociates from the lipoprotein if the appropriate binding site on ApoB is not found. The transience of the PCSK9-lipid interaction would explain why a one-site binding curve characteristic of a protein-protein interaction is obtained for the PCSK9-LDL interaction without being affected by lipid-docking. Further experiments studying long-term incubation of A44P-PCSK9 with LDL may elucidate whether PCSK9 is eventually able to bind ApoB without the help of a lipid-docking mechanism.

To summarize, the model that emerges based on our results posits that free PCSK9 in the circulation has a disordered, solvent exposed prodomain N-terminal which forms a lipid-ordered helix in proximity to the surface of a lipoprotein. The amphipathic nature of the helix allows PCSK9 to dock onto the phospholipid exterior and scan the surface for the PCSK9 binding site on ApoB. Once the binding site is found, a stable protein-protein interaction is formed. Whether this binding site is located in the N-terminal region or elsewhere remains to be determined. If the binding site is not found, the PCSK9 will dissociate from the lipoprotein (Figure 14).

4.3 The R46L polymorphism and LDL

The mechanism of loss-of-function in PCSK9 variants is of interest for the purposes of therapeutic development. The R46L polymorphism of PCSK9 is a well-studied variant of PCSK9, common in European Caucasian descendants, associated with significantly lowered levels of plasma LDL-cholesterol and lowered risk for heart disease[67, 74, 75]. The mechanism of the loss-of-function phenotype of R46L has only been partially elucidated. The lowered

circulating LDL-cholesterol levels have been found to be associated with a 15% decrease in circulating PCSK9 levels in healthy male R46L carriers[74, 82]. As well, R46L seems to be more susceptible to proteolysis, possibly due to decreased phosphorylation at the S47 position[52]. The lower levels of functioning circulating PCSK9 presumably lead to lower levels of LDLR degradation and better LDL-cholesterol clearance from plasma.

Substitution of an arginine with a leucine extends the conserved hydrophobic stretch located within the prodomain N-terminal; it also causes an extension of the hydrophobic face of the suggested N-terminal helix. Thus, we investigated the possibility that this polymorphism would show differential association with LDL, possibly contributing to its loss-of-function phenotype. Our in vitro work shows that R46L binds LDL with a similar affinity to wild-type PCSK9 (Figure 9), suggesting that differential LDL binding does not play a role in the loss-of-function mechanism of R46L-PCSK9. Further experiments in cell-culture or in vitro measuring the influence of LDL on the LDLR-degrading functionality of R46L-PCSK9 may be done to confirm this.

4.4 The regulation of PCSK9 activity by LDL

In cell culture, the presence of LDL has been shown to be inhibitory to the ability of PSCK9 to bind LDLR and undergo LDLR-dependent cellular uptake, independent of the LDL-LDLR interaction. LDL has also been shown to decrease the ability of PCSK9 to mediate LDLR degradation[6, 83]. As discussed in the introduction, this inhibition does not occur through a competition for, or steric inhibition of, a common binding site on PCSK9. PCSK9 is capable of binding to both LDL and the EGF-A domain of LDLR simultaneously in in vitro agarose gel shift assays[6]. However, the effect of LDL on the affinity of PCSK9 for the LDLR EGF-A

domain has not been measured. It is possible that LDL-bound PCSK9 experiences a change in affinity for the EGF-A domain of the LDLR or that the PCSK9-LDL interaction interferes with secondary contacts that may form between other regions of PCSK9, such as the C-terminal domain.

The N-terminal domain of the PCSK9 prodomain, required for the PCSK9-LDL interaction[6], is auto inhibitory to the LDLR binding and degrading function of PCSK9. Previous studies have found that deletion of the N-terminal region increased the affinity of PCSK9 for the extracellular domain of LDLR by 7-fold in vitro[25], while deletion of the acidic stretch of residues within the N-terminal domain led to a 30% decrease in LDL internalization in HepG2 cells expressing transfected PCSK9[60]. These findings form the basis of our hypothesis that the N-terminal region of the PCSK9 prodomain has a role in an allosteric mechanism, which regulates PCSK9 activity upon LDL-binding. Our findings suggested that a lipid-associating N-terminal α-helix may have a role in LDL-association and led us to test whether disruption of the helix would decrease the ability of PCSK9 to be regulated by LDL in cell culture. Our results confirm the previously observed inhibition of LDLR-mediated PCSK9 cellular uptake in the presence of LDL. However, we observed a minimal loss of PCSK9-LDLR binding inhibition by LDL both for deletion of the N-terminal region (Δ53-PCSK9) as well as helix disruption (A44P-PCSK9), despite normal association of PCSK9 with LDL under experimental conditions (Figure 13). We did note that the inhibition of wild-type PCSK9 uptake with LDL was not as strong in our assay as would be expected from literature[6], possibly resulting from differences in cell-line or assay conditions. Thus, further experiments in different cell culture conditions, as well as *in vivo*, may further elucidate the role of the N-terminal in the regulation of PCSK9 by LDL.

The overall working model that emerges regarding the PCSK9-LDL interaction posits that PCSK9 bound to LDL may form a pool of auto-inhibited PCSK9 in the circulation, in equilibrium with non-LDL bound active PCSK9, which is available for LDLR binding and degradation. Through this equilibrium, a steady state in healthy humans is achieved where rates of hepatic cholesterol production and PCSK9 secretion are balanced with PCSK9 clearance through LDLR-mediated endocytosis and LDLR degradation as well as LDLR-mediated plasma LDL clearance. As explained in a recent review[65], higher circulating levels of LDL in hypercholesterolemia may shift the equilibrium towards a larger pool of bound and inactive PCSK9. However, hypercholesterolemic patients also exhibit higher PCSK9 levels, as well as increases in PCSK9 due to statin treatment[84]. Given that the affinity of PCSK9 for LDL is only 325 nM, enough free PCSK9 should remain in the circulation to mediate high levels of LDLR degradation[6, 65].

4.5 Future directions

In the current study, we have presented evidence for a lipid-ordered helix in the N-terminal prodomain of PCSK9 that potentially plays a role in regulating the activity of PCSK9 through LDL-association. However, many aspects of this novel concept remain to be explored.

Structural information on the prodomain N-terminal is currently lacking due to the disordered nature of the region in crystallographic studies. Structural studies of the PCSK9 prodomain N-terminal in aqueous versus hydrophobic conditions would provide the strongest evidence regarding the ability of the N-terminal to form a lipid associating helix. We hope to conduct these investigations on peptide fragments of the N-terminal using techniques such as NMR

and circular dichroism. We also found that PCSK9 is capable of associating with lipids, which opens a new aspect of PCSK9 for exploration. Lipid and liposome binding studies using a variety of lipid compositions and particle sizes can be done to investigate the impact the lipid surface has on the binding capabilities of PCSK9.

As discussed earlier, the requirement of the prodomain N-terminal for binding to LDL does not guarantee that the actual binding site of ApoB lies in that region. Since LDL does not sterically inhibit the PCSK9-LDLR EGF-A interaction on the catalytic domain[25] it is most likely that if an alternate binding site for ApoB exists on PCSK9 it will be in the C-terminal domain. Further mapping, mutagenesis and binding studies can be carried out to investigate the potential of the C-terminal domain of PCSK9 as an ApoB binding site or as a regulatory domain.

Importantly, the development of the A44P-PCSK9 mutation, which shows ~90% decreased binding to LDL with no impact on LDLR-binding or degradation, presents an avenue for future in vivo studies of PCSK9 function independent of LDL-binding effects. The identification and characterization of the LDL-binding defective PCSK9-A44P will make it possible to distinguish direct and indirect effects of elevated LDL-cholesterol on circulating PCSK9 activity in mouse models of atherosclerosis. The PCSK9-LDL interaction has so far been studied only in in vitro and cell-culture contexts, and in vivo studies are the next step in definitively determining the effect of LDL association on PCSK9 function.

4.6 Conclusions

The emergence of PCSK9 as a safe therapeutic target for hypercholesterolemia treatment has opened a new era of research into PCSK9 biology and development of novel approaches to lower blood-cholesterol levels. The discovery that in addition to binding and directing LDLR degradation, PCSK9 is bound and inhibited by LDL particles themselves introduced a new aspect of PCSK9 regulation to be studied. The current study has investigated structural requirements for the PCSK9-LDL interaction within the autoinhibitory N-terminal region of the PCSK9 prodomain. Evidence was found for an amphipathic helix forming in the N-terminal region in proximity to lipid surfaces, and playing an important role in the ability of PCSK9 to bind LDL. Evidence was also found for the ability of PCSK9 to associate with liposomes. We further investigated the role these structural requirements play in the regulation of PCSK9 activity by LDL. Modest evidence was found that lack of the N-terminal region or potential disruption of the putative helix affected the ability of LDL to inhibit the PCSK9-LDLR interaction. Future studies will further elucidate the conformational changes that occur in the prodomain N-terminal region in aqueous and lipid environments, the role these conformations play in the regulation of PCSK9 activity, and the protein-protein interaction site where ApoB associates with PCSK9. Knowledge about the natural inhibition of PCSK9 activity by LDL will further inform efforts to create novel anti-PCSK9 hypercholesterolemia therapeutics.

5. References

1. Public Health Agency of Canada. Tracking heart disease and stroke in canada. Canada: Public Health Agency of Canada; 2009.

2. GBD 2013 Mortality and Causes of Death Collaborators. Global, regional, and national age-sex specific all-cause and cause-specific mortality for 240 causes of death, 1990-2013: A systematic analysis for the global burden of disease study 2013. Lancet 2015 Jan 10;385(9963):117-71.

3. Beltowski J, Wojcicka G, Jamroz-Wisniewska A. Adverse effects of statins - mechanisms and consequences. Curr Drug Saf 2009 Sep;4(3):209-28.

4. Abifadel M, Varret M, Rabes J, Allard D, Ouguerram K, Devillers M, Cruaud C, Benjannet S, Wickham L, Erlich D, et al. Mutations in PCSK9 cause autosomal dominant hypercholesterolemia. Nat Genet 2003 06;34(2):154.

5. Stein EA, Swergold GD. Potential of proprotein convertase subtilisin/kexin type 9 based therapeutics. Curr Atheroscler Rep 2013 Mar;15(3):310,013-0310-3.

6. Kosenko T, Golder M, Leblond G, Weng W, Lagace TA. Low density lipoprotein binds to proprotein convertase subtilisin/kexin type-9 (PCSK9) in human plasma and inhibits PCSK9-mediated low density lipoprotein receptor degradation. J Biol Chem 2013 Mar 22;288(12):8279-88.

7. Sun H, Samarghandi A, Zhang N, Yao Z, Xiong M, Teng BB. Proprotein convertase subtilisin/kexin type 9 interacts with apolipoprotein B and prevents its intracellular degradation, irrespective of the low-density lipoprotein receptor. Arterioscler Thromb Vasc Biol 2012 Jul;32(7):1585-95.

8. Tavori H, Fan D, Blakemore JL, Yancey PG, Ding L, Linton MF, Fazio S. Serum proprotein convertase subtilisin/kexin type 9 and cell surface low-density lipoprotein receptor: Evidence for a reciprocal regulation. Circulation 2013 Jun 18;127(24):2403-13.

9. Voet D, Voet JG. Biochemistry. 3rd ed ed. United States of America: Wiley; 2004. .

10. Brown MS, Goldstein JL. The SREBP pathway: Regulation of cholesterol metabolism by proteolysis of a membrane-bound transcription factor. Cell 1997 May 2;89(3):331-40.

11. Sharpe LJ, Brown AJ. Controlling cholesterol synthesis beyond 3-hydroxy-3-methylglutaryl-CoA reductase (HMGCR). J Biol Chem 2013 Jun 28;288(26):18707-15.

12. Gill S, Stevenson J, Kristiana I, Brown AJ. Cholesterol-dependent degradation of squalene monooxygenase, a control point in cholesterol synthesis beyond HMG-CoA reductase. Cell Metab 2011 Mar 2;13(3):260-73.

13. Ramasamy I. Recent advances in physiological lipoprotein metabolism. Clin Chem Lab Med 2014 Dec;52(12):1695-727.

14. Sviridov D, Nestel P. Dynamics of reverse cholesterol transport: Protection against atherosclerosis. Atherosclerosis 2002;161(2):245-54.

15. Hevonoja T, Pentikainen MO, Hyvonen MT, Kovanen PT, Ala-Korpela M. Structure of low density lipoprotein (LDL) particles: Basis for understanding molecular changes in modified LDL. Biochim Biophys Acta 2000 Nov 15;1488(3):189-210.

16. Krauss RM, Burke DJ. Identification of multiple subclasses of plasma low density lipoproteins in normal humans. J Lipid Res 1982 Jan;23(1):97-104.

17. Otvos JD, Jeyarajah EJ, Cromwell WC. Measurement issues related to lipoprotein heterogeneity. Am J Cardiol 2002 10/17;90(8, Supplement):22-9.

18. Austin MA, Breslow JL, Hennekens CH, Buring JE, Willett WC, Krauss RM. Low-density lipoprotein subclass patterns and risk of myocardial infarction. JAMA 1988 Oct 7;260(13):1917-21.

19. Boren J, Lee I, Zhu W, Arnold K, Taylor S, Innerarity TL. Identification of the low density lipoprotein receptor-binding site in apolipoprotein B100 and the modulation of its binding activity by the carboxyl terminus in familial defective apo-B100. J Clin Invest 1998 Mar 1;101(5):1084-93.

20. Segrest JP, Jones MK, Mishra VK, Anantharamaiah GM, Garber DW. apoB-100 has a pentapartite structure composed of three amphipathic alpha-helical domains alternating with two amphipathic beta-strand domains. detection by the computer program LOCATE. Arterioscler Thromb 1994 Oct;14(10):1674-85.

21. Segrest JP, Jones MK, De Loof H, Dashti N. Structure of apolipoprotein B-100 in low density lipoproteins. J Lipid Res 2001 Sep;42(9):1346-67.

22. He G, Gupta S, Yi M, Michaely P, Hobbs HH, Cohen JC. ARH is a modular adaptor protein that interacts with the LDL receptor, clathrin, and AP-2. J Biol Chem 2002 Nov 15;277(46):44044-9.

23. Davis CG, van Driel IR, Russell DW, Brown MS, Goldstein JL. The low density lipoprotein receptor. identification of amino acids in cytoplasmic domain required for rapid endocytosis. J Biol Chem 1987 Mar 25;262(9):4075-82.

24. Gent J, Braakman I. Low-density lipoprotein receptor structure and folding. Cell Mol Life Sci 2004 Oct;61(19-20):2461-70.

25. Kwon HJ, Lagace TA, McNutt MC, Horton JD, Deisenhofer J. Molecular basis for LDL receptor recognition by PCSK9. Proc Natl Acad Sci U S A 2008 Feb 12;105(6):1820-5.

26. Anderson RGW, Brown MS, Goldstein JL. Role of the coated endocytic vesicle in the uptake of receptor-bound low density lipoprotein in human fibroblasts. Cell 1977 3;10(3):351-64.

27. Brown MS, Kovanen PT, Goldstein JL. Regulation of plasma cholesterol by lipoprotein receptors. Science 1981 May 8;212(4495):628-35.

28. Brown MS, Anderson RG, Goldstein JL. Recycling receptors: The round-trip itinerary of migrant membrane proteins. Cell 1983 Mar;32(3):663-7.

29. Horton JD, Shimomura I, Brown MS, Hammer RE, Goldstein JL, Shimano H. Activation of cholesterol synthesis in preference to fatty acid synthesis in liver and adipose tissue of transgenic mice overproducing sterol regulatory element-binding protein-2. J Clin Invest 1998 Jun 1;101(11):2331-9.

30. Brown AJ, Sun L, Feramisco JD, Brown MS, Goldstein JL. Cholesterol addition to ER membranes alters conformation of SCAP, the SREBP escort protein that regulates cholesterol metabolism. Mol Cell 2002 Aug;10(2):237-45.

31. Sato R, Inoue J, Kawabe Y, Kodama T, Takano T, Maeda M. Sterol-dependent transcriptional regulation of sterol regulatory element-binding protein-2. J Biol Chem 1996 Oct 25;271(43):26461-4.

32. National Cholesterol Education Program (NCEP) Expert Panel on Detection, Evaluation, and Treatment of High Blood Cholesterol in Adults (Adult Treatment Panel III). Third report of the national cholesterol education program (NCEP) expert panel on detection, evaluation, and treatment of high blood cholesterol in adults (adult treatment panel III) final report. Circulation 2002 Dec 17;106(25):3143-421.

33. Williams KJ, Tabas I. The response-to-retention hypothesis of early atherogenesis. Arterioscler Thromb Vasc Biol 1995 May;15(5):551-61.

34. Tabas I, Williams KJ, Boren J. Subendothelial lipoprotein retention as the initiating process in atherosclerosis: Update and therapeutic implications. Circulation 2007 Oct 16;116(16):1832-44.

35. Williams KJ, Tabas I. The response-to-retention hypothesis of atherogenesis reinforced. Curr Opin Lipidol 1998 Oct;9(5):471-4.

36. Libby P, Ridker PM, Hansson GK. Progress and challenges in translating the biology of atherosclerosis. Nature 2011 May 19;473(7347):317-25.

37. Lambert G, Sjouke B, Choque B, Kastelein JJ, Hovingh GK. The PCSK9 decade. J Lipid Res 2012 Dec;53(12):2515-24.

38. Goldstein JL, Brown MS. The LDL receptor. Arterioscler Thromb Vasc Biol 2009 Apr;29(4):431-8.

39. Goldstein JL, Brown MS. Regulation of the mevalonate pathway. Nature 1990 Feb 1;343(6257):425-30.

40. Buhaescu I, Izzedine H. Mevalonate pathway: A review of clinical and therapeutical implications. Clin Biochem 2007 Jun;40(9-10):575-84.

41. Golomb BA, Evans MA. Statin adverse effects : A review of the literature and evidence for a mitochondrial mechanism. Am J Cardiovasc Drugs 2008;8(6):373-418.

42. Abd TT, Jacobson TA. Statin-induced myopathy: A review and update. Expert Opin Drug Saf 2011 May;10(3):373-87.

43. Seidah NG, Benjannet S, Wickham L, Marcinkiewicz J, Jasmin SB, Stifani S, Basak A, Prat A, Chretien M. The secretory proprotein convertase neural apoptosis-regulated convertase 1 (NARC-1): Liver regeneration and neuronal differentiation. Proc Natl Acad Sci U S A 2003 Feb 4;100(3):928-33.

44. Seidah NG, Prat A. The biology and therapeutic targeting of the proprotein convertases. Nat Rev Drug Discov 2012 May;11(5):367-83.

45. Henrich S, Lindberg I, Bode W, Than ME. Proprotein convertase models based on the crystal structures of furin and kexin: Explanation of their specificity. J Mol Biol 2005 Jan 14;345(2):211-27.

46. Cunningham D, Danley DE, Geoghegan KF, Griffor MC, Hawkins JL, Subashi TA, Varghese AH, Ammirati MJ, Culp JS, Hoth LR, et al. Structural and biophysical studies of PCSK9 and its mutants linked to familial hypercholesterolemia. Nat Struct Mol Biol 2007 May;14(5):413-9.

47. Piper DE, Jackson S, Liu Q, Romanow WG, Shetterly S, Thibault ST, Shan B, Walker NPC. The crystal structure of PCSK9: A regulator of plasma LDL-cholesterol. Structure 2007 5/16;15(5):545-52.

48. Hampton EN, Knuth MW, Li J, Harris JL, Lesley SA, Spraggon G. The self-inhibited structure of full-length PCSK9 at 1.9 A reveals structural homology with resistin within the C-terminal domain. Proc Natl Acad Sci U S A 2007 Sep 11;104(37):14604-9.

49. Du F, Hui Y, Zhang M, Linton MF, Fazio S, Fan D. Novel domain interaction regulates secretion of proprotein convertase subtilisin/kexin type 9 (PCSK9) protein. J Biol Chem 2011 Dec 16;286(50):43054-61.

50. Chen XW, Wang H, Bajaj K, Zhang P, Meng ZX, Ma D, Bai Y, Liu HH, Adams E, Baines A, et al. SEC24A deficiency lowers plasma cholesterol through reduced PCSK9 secretion. Elife 2013 Apr 9;2:e00444.

51. Benjannet S, Rhainds D, Essalmani R, Mayne J, Wickham L, Jin W, Asselin MC, Hamelin J, Varret M, Allard D, et al. NARC-1/PCSK9 and its natural mutants: Zymogen cleavage and effects on the low density lipoprotein (LDL) receptor and LDL cholesterol. J Biol Chem 2004 Nov 19;279(47):48865-75.

52. Dewpura T, Raymond A, Hamelin J, Seidah NG, Mbikay M, Chretien M, Mayne J. PCSK9 is phosphorylated by a golgi casein kinase-like kinase ex vivo and circulates as a phosphoprotein in humans. FEBS J 2008 Jul;275(13):3480-93.

53. Park SW, Moon YA, Horton JD. Post-transcriptional regulation of low density lipoprotein receptor protein by proprotein convertase subtilisin/kexin type 9a in mouse liver. J Biol Chem 2004 Nov 26;279(48):50630-8.

54. Maxwell KN, Breslow JL. Adenoviral-mediated expression of Pcsk9 in mice results in a low-density lipoprotein receptor knockout phenotype. Proc Natl Acad Sci U S A 2004 May 4;101(18):7100-5.

55. Lagace TA, Curtis DE, Garuti R, McNutt MC, Park SW, Prather HB, Anderson NN, Ho YK, Hammer RE, Horton JD. Secreted PCSK9 decreases the number of LDL receptors in hepatocytes and in livers of parabiotic mice. J Clin Invest 2006 Nov;116(11):2995-3005.

56. Grefhorst A, McNutt MC, Lagace TA, Horton JD. Plasma PCSK9 preferentially reduces liver LDL receptors in mice. J Lipid Res 2008 Jun;49(6):1303-11.

57. Zhang DW, Garuti R, Tang WJ, Cohen JC, Hobbs HH. Structural requirements for PCSK9-mediated degradation of the low-density lipoprotein receptor. Proc Natl Acad Sci U S A 2008 Sep 2;105(35):13045-50.

58. McNutt MC, Lagace TA, Horton JD. Catalytic activity is not required for secreted PCSK9 to reduce low density lipoprotein receptors in HepG2 cells. J Biol Chem 2007 Jul 20;282(29):20799-803.

59. Leren TP. Sorting an LDL receptor with bound PCSK9 to intracellular degradation. Atherosclerosis 2014 11;237(1):76-81.

60. Holla OL, Laerdahl JK, Strom TB, Tveten K, Cameron J, Berge KE, Leren TP. Removal of acidic residues of the prodomain of PCSK9 increases its activity towards the LDL receptor. Biochem Biophys Res Commun 2011 Mar 11;406(2):234-8.

61. Nguyen MA, Kosenko T, Lagace TA. Internalized PCSK9 dissociates from recycling LDL receptors in PCSK9-resistant SV-589 fibroblasts. J Lipid Res 2014 Feb;55(2):266-75.

62. Seidah NG, Poirier S, Denis M, Parker R, Miao B, Mapelli C, Prat A, Wassef H, Davignon J, Hajjar KA, et al. Annexin A2 is a natural extrahepatic inhibitor of the PCSK9-induced LDL receptor degradation. PLoS One 2012 Jul 27;7(7):. doi:10.1371/journal.pone.0041865.

63. Dubuc G, Chamberland A, Wassef H, Davignon J, Seidah NG, Bernier L, Prat A. Statins upregulate PCSK9, the gene encoding the proprotein convertase neural apoptosis-regulated convertase-1 implicated in familial hypercholesterolemia. Arterioscler Thromb Vasc Biol 2004 Aug;24(8):1454-9.

64. Li H, Dong B, Park SW, Lee HS, Chen W, Liu J. Hepatocyte nuclear factor 1alpha plays a critical role in PCSK9 gene transcription and regulation by the natural hypocholesterolemic compound berberine. J Biol Chem 2009 Oct 16;284(42):28885-95.

65. Lagace TA. PCSK9 and LDLR degradation: Regulatory mechanisms in circulation and in cells. Curr Opin Lipidol 2014 Oct;25(5):387-93.

66. Cohen J, Pertsemlidis A, Kotowski IK, Graham R, Garcia CK, Hobbs HH. Low LDL cholesterol in individuals of african descent resulting from frequent nonsense mutations in PCSK9. Nat Genet 2005 Feb;37(2):161-5.

67. Cohen JC, Boerwinkle E, Mosley TH, Hobbs HH. Sequence variations in PCSK9, low LDL, and protection against coronary heart disease. N Engl J Med 2006 03/23; 2015/01;354(12):1264-72.

68. Zhao Z, Tuakli-Wosornu Y, Lagace TA, Kinch L, Grishin NV, Horton JD, Cohen JC, Hobbs HH. Molecular characterization of loss-of-function mutations in PCSK9 and identification of a compound heterozygote. Am J Hum Genet 2006 Sep;79(3):514-23.

69. Hooper AJ, Marais AD, Tanyanyiwa DM, Burnett JR. The C679X mutation in PCSK9 is present and lowers blood cholesterol in a southern african population. Atherosclerosis 2007 8;193(2):445-8.

70. Russell DW, Brown MS, Goldstein JL. Different combinations of cysteine-rich repeats mediate binding of low density lipoprotein receptor to two different proteins. J Biol Chem 1989 Dec 25;264(36):21682-8.

71. HAVEL RJ, EDER HA, BRAGDON JH. The distribution and chemical composition of ultracentrifugally separated lipoproteins in human serum. J Clin Invest 1955 Sep;34(9):1345-53.

72. Peterson GL. A simplification of the protein assay method of lowry et al. which is more generally applicable. Anal Biochem 1977 Dec;83(2):346-56.

73. Yee MS, Pavitt DV, Tan T, Venkatesan S, Godsland IF, Richmond W, Johnston DG. Lipoprotein separation in a novel iodixanol density gradient, for composition, density, and phenotype analysis. J Lipid Res 2008 Jun;49(6):1364-71.

74. Humphries SE, Neely RD, Whittall RA, Troutt JS, Konrad RJ, Scartezini M, Li KW, Cooper JA, Acharya J, Neil A. Healthy individuals carrying the PCSK9 p.R46L variant and familial hypercholesterolemia patients carrying PCSK9 p.D374Y exhibit lower plasma concentrations of PCSK9. Clin Chem 2009 Dec;55(12):2153-61.

75. Kotowski IK, Pertsemlidis A, Luke A, Cooper RS, Vega GL, Cohen JC, Hobbs HH. A spectrum of PCSK9 alleles contributes to plasma levels of low-density lipoprotein cholesterol. Am J Hum Genet 2006 Mar;78(3):410-22.

76. Hobbs HH, Brown MS, Goldstein JL. Molecular genetics of the LDL receptor gene in familial hypercholesterolemia. Hum Mutat 1992;1(6):445-66.

77. Fan D, Yancey PG, Qiu S, Ding L, Weeber EJ, Linton MF, Fazio S. Self-association of human PCSK9 correlates with its LDLR-degrading activity. Biochemistry 2008 Feb 12;47(6):1631-9.

78. Luo Y, Warren L, Xia D, Jensen H, Sand T, Petras S, Qin W, Miller KS, Hawkins J. Function and distribution of circulating human PCSK9 expressed extrahepatically in transgenic mice. J Lipid Res 2009 Aug;50(8):1581-8.

79. Johnson JE, Cornell RB. Membrane-binding amphipathic alpha-helical peptide derived from CTP:Phosphocholine cytidylyltransferase. Biochemistry 1994 Apr 12;33(14):4327-35.

80. Bhattacharyya R, Chakrabarti P. Stereospecific interactions of proline residues in protein structures and complexes. J Mol Biol 2003 Aug 22;331(4):925-40.

81. Thiam AR, Farese RV,Jr, Walther TC. The biophysics and cell biology of lipid droplets. Nat Rev Mol Cell Biol 2013 Dec;14(12):775-86.

82. Lakoski SG, Lagace TA, Cohen JC, Horton JD, Hobbs HH. Genetic and metabolic determinants of plasma PCSK9 levels. J Clin Endocrinol Metab 2009 Jul;94(7):2537-43.

83. Fisher TS, Lo Surdo P, Pandit S, Mattu M, Santoro JC, Wisniewski D, Cummings RT, Calzetta A, Cubbon RM, Fischer PA, et al. Effects of pH and low density lipoprotein

(LDL) on PCSK9-dependent LDL receptor regulation. J Biol Chem 2007 Jul 13;282(28):20502-12.

84. Raal F, Panz V, Immelman A, Pilcher G. Elevated PCSK9 levels in untreated patients with heterozygous or homozygous familial hypercholesterolemia and the response to high-dose statin therapy. J Am Heart Assoc 2013 Apr 24;2(2):e000028.

85. Takahashi N, Hamada-Nakahara S, Itoh Y, Takemura K, Shimada A, Ueda Y, Kitamata M, Matsuoka R, Hanawa-Suetsugu K, Senju Y, et al. TRPV4 channel activity is modulated by direct interaction of the ankyrin domain to PI(4,5)P(2). Nat Commun 2014 Sep 26;5:4994.